The intracellular symbiont *Wolbachia* alters *Drosophila* development and metabolism to buffer against nutritional stress

Amelia RI Lindsey[1*], Jason M Tennessen[2], Michael A Gelaw[1], Megan W Jones[1], Audrey J Parish[2], Irene LG Newton[2], Travis Nemkov[3], Angelo D'Alessandro[3], Madhulika Rai[2], Nicole Stark[2]

[*]To whom correspondence should be addressed (alindsey@umn.edu)

[1]Department of Entomology, University of Minnesota, St. Paul, Minnesota, USA

[2]Department of Biology, Indiana University, Bloomington, Indiana, USA

[3]Department of Biochemistry and Molecular Genetics, University of Colorado Anschutz Medical Campus, Colorado, USA

ORCIDs:

ARIL: 0000-0003-3354-7419

JMT: 0000-0002-3527-5683

AJP: 0000-0002-8127-3769

ILGN: 0000-0002-7118-0374

TN: 0000-0001-8566-7119

ADA: 0000-0002-2258-6490

MR: 0000-0003-0228-285X

Short Title:

***Wolbachia* buffers against nutritional stress**

ABSTRACT

The intracellular bacterium *Wolbachia* is a common symbiont of many arthropods and nematodes, well studied for its impacts on host reproductive biology. However, its broad success as a vertically transmitted infection cannot be attributed to manipulations of host reproduction alone. Using the *Drosophila melanogaster* model and their natively associated *Wolbachia* strain "*w*Mel", we show that *Wolbachia* infection supports fly development and buffers against nutritional stress. *Wolbachia* infection across several fly genotypes and a range of nutrient conditions resulted in reduced pupal mortality, increased adult emergence, and larger size. We determined that the exogenous supplementation of pyrimidines partially rescued developmental phenotypes in the *Wolbachia*-free flies, and that *Wolbachia* titers were responsive to reduced gene expression of the fly's *de novo* pyrimidine synthesis pathway. In parallel, transcriptomic and metabolomic analyses indicated that *Wolbachia* impacts larval biology far beyond pyrimidine metabolism. *Wolbachia*-infected larvae had strong signatures of shifts in glutathione and mitochondrial metabolism, plus significant changes in the expression of key developmental regulators including *Notch*, the insulin receptor (*InR*), and the juvenile hormone receptor *Methoprene-tolerant* (*Met*). We propose that *Wolbachia* acts as a beneficial symbiont to support fly development and enhance host fitness, especially during periods of nutrient stress.

SIGNIFICANCE

Wolbachia is a bacterial symbiont of arthropods and nematodes, well described for its manipulations of arthropod reproduction. However, many have theorized there must be more to this symbiosis, even in well-studied *Wolbachia*-host relationships such as with *Drosophila*. Reproductive impacts alone cannot explain the success and ubiquity of this bacterium. Here, we use *Drosophila melanogaster* and their native *Wolbachia* infections to show that *Wolbachia* supports fly development and significantly buffers flies against nutritional stress. These developmental advantages might help explain the ubiquity of *Wolbachia* infections.

INTRODUCTION

Maternally transmitted microbes have evolved numerous ways to alter host biology, ultimately facilitating their own transmission. Strategies include supplementation of the host's diet via nutrient provisioning, protection against parasites and infections, and even direct manipulation of host reproduction (1). Many insects, other terrestrial arthropods, and some nematode species are infected with bacteria in the genus *Wolbachia* (Alphaproteobacteria: Rickettsiales), a maternally transmitted infection long appreciated for its direct impacts on host reproduction and sex ratios (1-10). Critically, *Wolbachia* can spread through populations in the absence of such reproductive manipulations (11). And, increasingly, other *Wolbachia*-mediated benefits to the host are being uncovered (12). For example, a suite of *Wolbachia* strains can protect host insects against secondary infections, especially viruses, a phenomenon that now forms the basis of many ongoing vector control programs across the world (13, 14). Certain strains of *Wolbachia* are obligate beneficial nutritional symbionts, such as the bed bug-infecting *Wolbachia* that produce B-vitamins to support their obligately hematophagous hosts (15). In other insects, facultative associations with *Wolbachia* have likewise been implicated in the balance of cholesterol, iron, or B-vitamins (16-19).

We previously identified that *Wolbachia* infection results in a suite of changes to the expression of *Drosophila melanogaster* nucleotide metabolism pathways (20). Additionally, comparative genomic data indicate that the biosynthetic pathways for the *de novo* synthesis of purines and pyrimidines have been conserved across *Wolbachia*, pointing towards their broad importance (21). Furthermore, *Wolbachia* encode for an abundance of amino acid importers, which would provide necessary precursors for *Wolbachia*'s *de novo* synthesis of nucleotides (3, 21). The conservation of these metabolic pathways might simply represent essential functions for *Wolbachia*'s own metabolism, or they might also be important in the context of interaction with the host.

While there are increasing examples in the literature that hint at significant metabolic interplay between *Wolbachia* and hosts, our understanding of the symbiosis is still largely focused on reproductive processes and other aspects of adult biology (1). Indeed, we know very little about *Wolbachia*'s interactions with hosts during development. In insects, not only is the juvenile period physiologically distinct (especially in holometabolous insects that undergo complete metamorphosis) but also this developmental period determines many aspects of adult biology and fitness (22-24). To address this significant gap in knowledge, we undertook a series of experiments using the fruit fly, *Drosophila melanogaster*, naturally infected with the *Wolbachia* strain *w*Mel. We hypothesized that *Wolbachia* plays a supporting role in host nutrition, and used a combination of transcriptomics, metabolomics, diet manipulations, and fly genetics to investigate the relationship between developing flies and their *Wolbachia* infections.

METHODS

Fly husbandry

Drosophila melanogaster stocks with or without their native *Wolbachia* strain "*w*Mel" were maintained on standard Bloomington cornmeal-agar medium at 25 °C on a 24-hour, 12:12 light:dark cycle under density-controlled conditions and 50% relative humidity. *Wolbachia* colonization status was confirmed with PCR assays using *Wolbachia*-specific 16S primers WspecF and WspecR (25). Genotypes used in nutritional assays (below) included: DGRP-320 (RRID:BDSC_29654), a *Wolbachia*-infected isogenic wild-type strain with genome sequence available which we refer to as "wild-type" below (26), and a *Wolbachia*-infected white line, w^{145} (RRID:BDSC_145). *Wolbachia*-cleared counterpart stocks were generated with antibiotics via three generations of tetracycline treatment (20 µg/mL in the fly food for three generations), followed by re-inoculation of the gut microbiome by transfer to bottles that previously harbored male flies from the original stock that had fed and defecated on the media for one week (27).

105 Stocks were allowed to recover from any potential transgenerational effects of the antibiotic
106 treatment for at least an additional ten generations prior to use in any experiment and re-screened
107 for *Wolbachia* infection immediately prior to all experiments. All other fly stocks (e.g., RNAi lines),
108 are detailed in Supplementary Table S1.
109
110 RNA-Seq of larvae
111 Pools of second instar ("L2") DGRP-320 larvae with or without *Wolbachia* were processed for
112 transcriptomic analyses. For each infection status, three vials were initiated by allowing five pairs
113 of adult flies per vial to mate and lay eggs on standard Bloomington cornmeal-agar medium for 8
114 hours. After this period, the adults were removed, and larvae were maintained under standard
115 rearing conditions. Flies were allowed to develop until the L2 stage, at which point they were
116 removed from each vial with a dissecting pin and transferred to a microcentrifuge tube containing
117 sterile 1X phosphate buffered saline (PBS). Each pool of 20 L2s was washed three times with 1X
118 PBS, after which the solution was removed, and larvae were flash frozen in liquid nitrogen. Total
119 RNA was extracted from each pool using the Monarch® Total RNA Miniprep Kit (New England
120 Biolabs) including on-column DNase treatment. RNA-seq libraries were prepared by Novogene
121 Co, Ltd. and followed a standard strand-specific Illumina-compatible preparation (New England
122 Biolabs) including purification of mRNA using oligo-dT beads. Libraries were sequenced on an
123 Illumina NovaSeq platform to generate ~9Gb of paired end 150bp reads per library. Reads were
124 mapped to extracted reference transcripts of the *Drosophila melanogaster* reference genome
125 (release 6.48) (28) using the RSEM v. 1.3.0 (29) programs 'rsem-prepare-reference' and 'rsem-
126 calculate-expression', employing the STAR v. 2.3.5a aligner (30). Transcript abundance was
127 summarized and imported to R v. 4.3.0 (31) with tximport v. 1.28.0 (32) for use in downstream
128 analyses. Only genes with >1 count per million in at least two samples were retained for analysis.
129 Differential gene expression was assessed with EdgeR v. 3.42.4 (33, 34), employing a TMM
130 normalization, dispersion calculation, and a generalized linear model, with quasi-likelihood F-tests

131 (function 'glmQLFit'). Genes that were significantly differentially expressed were defined as those
132 with a false discovery rate (FDR) q-value of <0.05. Mitochondrial genes in the DEG dataset were
133 extracted along with their annotations in mitoXplorer 2.0 (35, 36). We determined enrichment with
134 PANGEA (37) using all DEGs as the test set, all expressed genes (Supplemental Table S3) as
135 the background, and gene set categories of 'KEGG Pathway D. mel', 'Preferred tissue
136 (modEncode RNA_seq)', and all three *Drosophila* GOslim gene sets (Biological Process, Cellular
137 Component, Molecular Function). Gene sets with p<0.05 after Benjamini & Hochberg corrections
138 for multiple testing, or >2 fold-change with uncorrected p-value of p<0.05 are displayed. DEGs
139 were also clustered into an interaction network using STRING v.1.4.2 (38), implemented in
140 Cytoscape v.3.6.0 (39), which simultaneously assesses overrepresentation of STRING clusters.
141 The confidence threshold for network building was set to 0.85 (i.e., highly stringent).
142
143 *Wolbachia* developmental transcriptomics
144 To assess *Wolbachia* gene expression, we analyzed the *Wolbachia* transcriptomes extracted from
145 the MODENCODE dataset (40, 41). This dataset has previously been used to find *Wolbachia*
146 genes that are significantly differentially expressed across fly development (40-42). Importantly,
147 and as those studies have noted, this is a large data set with limited power to detect differences
148 due to low replication across a very large number of stages that are not necessarily biologically
149 independent or strictly linearly correlated. As such, previously identified DEGs are primarily those
150 with large changes in expression and limited developmental stage-by-expression interactive
151 effects. To combat this challenge, we opted to take a genome-wide approach to look at these data
152 without the goal of identifying specific differentially expressed genes. The dataset was further
153 curated by removing tissue-specific libraries (e.g., L3 midguts), and averaging TPM values within
154 a developmental time point for those represented by multiple libraries. To assign orthology to each
155 *w*Mel protein, we used a previously constructed database (43) of proteins from 33 *Wolbachia*
156 genomes (representing nine Supergroups: A, B, C, D, E, F, J, L, T), clustered into orthologous

157 groups with ProteinOrtho v5.15 (44). We assessed each *w*Mel protein for phylogenetic
158 conservation as either a “core” or “unique” gene at a range of taxonomic levels. The “unique”
159 designation was for proteins that were found in all members of a given clade and also restricted
160 to that clade (i.e. not found in any other *Wolbachia* strains). The “core” designation was for
161 proteins that were present in all members of a clade without regard to their presence in other
162 strains outside of that clade. Using these assignments we designated the following groups of
163 *w*Mel proteins: (1) unique to *w*Mel, (2) core to the *Drosophila*-infecting clade within Supergroup A
164 (*w*Mel, *w*Ri, *w*Au, *w*Rec, *w*Ha, *w*Suz), (3) core to Supergroup A, (4) core to Supergroups A and B,
165 (5) core proteins across all *Wolbachia*, and, (6) all other *w*Mel proteins. Statistics and data
166 visualization were carried out in R version 4.1.3 (31). Expression clustering and visualization was
167 performed with R package ‘pheatmap’ (45) and clustering method ‘complete’. Functional
168 enrichment tests for *w*Mel gene sets were performed with ShinyGO 0.80 (46) using ‘Wolbachia
169 endosymbiont of Drosophila melanogaster’ (ID = ‘STRING.163164.Wolbachia’) as the species, a
170 custom background gene set of the 1191 expressed genes, GO Biological Process as the pathway
171 database, and an FDR cutoff of p = 0.05.
172
173 Nutritional stress experiments
174 To generate poor media, Nutri-fly® Bloomington Formulation (Genesee Scientific 66-121) was
175 prepared according to manufacturer’s instructions and diluted to indicated percentages while
176 maintaining the full concentrations of agar (5.3 g/L) and propionic acid (4.8 ml/L). Five ml of media
177 was aliquoted into each vial. Flies were placed in mating cages on grape agar plates streaked
178 with yeast paste and acclimated for 24 hours, prior to initiating 4-hour egg lays. Upon hatching, <
179 4-hour old L1 larvae were transferred to media vials (n=20 per vial), and development was scored
180 every 24 hours. Pupation was defined by eversion of the anterior spiracles (47). Each vial was
181 tracked until all flies eclosed, or until three consecutive days without additional adult emergence.
182

183 Axenic assays

184 To test if the gut microbiome was playing a role in *Wolbachia*-mediated developmental
185 phenotypes, we reared wild-type flies with and without *Wolbachia* on 100% and 25% strength
186 media under axenic conditions (i.e., without the gut or food microbiome). 10 mL of media
187 (prepared according to protocols in "nutritional stress experiments") was aliquoted into
188 polypropylene wide vials, capped with a Cellulose Acetate Flug® (Flystuff 49-101), and
189 autoclaved on liquid setting for 20 minutes to sterilize. Embryos were collected on grape agar with
190 yeast paste as described previously and transferred into 70-micron mesh cell strainers (Falcon
191 352350). Embryos in the cell strainers were washed with *Drosophila* embryo wash solution (7%
192 NaCl, 0.5% Triton X-100) to remove food debris. After an initial wash, embryos were immersed in
193 a 10% bleach solution for 3 minutes, with gentle mixing every 30 seconds. The embryos were
194 then washed with sterile *Drosophila* embryo wash solution to remove excess bleach. Embryos
195 were subjected to a final rinse with sterile phosphate buffered saline (PBS) and transferred to a
196 sterile agar culture plate (2% agar in deionized water) stained with blue gel food coloring to
197 facilitate counting. A flame-sterilized probe was used to transfer 20 embryos into each vial of
198 sterile media, and developmental assays were carried out as described above.

199

200 Nutritional supplementation experiments

201 To test the impact of specific nutrients, we prepared 12.5% strength media as above, and
202 selectively added in protein or nucleotides: the precursors and end points of *de novo* nucleotide
203 biosynthesis. Treatments included casein (for bulk addition of amino acids at 64.1 g/L; Sigma
204 C7078), inosine (0.74 g/L; Sigma I4125), uridine (0.67 g/L; Sigma U3003), or both inosine and
205 uridine at the aforementioned concentrations. The concentrations of additives were calculated as
206 87.5% of a previously defined holidic diet (48), to adjust for the 12.5% BDSC media strength.
207 Developmental assays were carried out as described above.

208

209 Pupal size measurements

210 After selected developmental assays, pupal casings and dead pupae were removed from vials
211 using a wet paint brush and transferred to glass slides. Pupae were imaged with brightfield
212 microscopy on an ECHO Revolve at 4X. Images were manually annotated in Echo Labs Pro
213 software to measure sizes. Pupal length was defined as the distance between the base of the
214 posterior spiracles to the midway point between the anterior spiracles. Width measurements were
215 taken at the widest part of the pupa. The volume of each pupa was calculated assuming a prolate
216 spheroid shape [$V = (4/3)\ \pi\ (\text{width}/2)^2\ (\text{length}/2)$] (Supplemental Figure S2) (49, 50). For assays
217 in which we sexed and measured pupae, we allowed five pairs of flies to mate and lay eggs on
218 the appropriate media for four days, after which the adults were cleared, and offspring were
219 allowed to develop under standard rearing conditions. Approximately 50 pupae per condition were
220 collected at pupal stages P13-14 (51), and sexed based on the presence of sex combs prior to
221 measurement.

222

223 Knockdown of fly nucleotide metabolism genes

224 *Wolbachia*-infected Transgenic RNAi Project ("TRiP") stocks were obtained from the Bloomington
225 *Drosophila* Stock Center to knock down expression of genes in the purine and pyrimidine
226 nucleotide biosynthesis pathways (Supplemental File S1). Unmated females carrying a UAS-
227 gene-specific short hairpin were crossed to males with an Act5C-Gal4 driver (RRID:BDSC_3954:
228 $y^1 w^*$; P{w^{+mC}=Act5C-GAL4}17bFO1/TM6B, Tb^1). Unmated, F1 female progeny were sorted as
229 adults into those with the short hairpin and Gal4-driver or those with the short hairpin and the
230 TM6B balancer. At three days old, the sorted flies were flash frozen in liquid nitrogen and then
231 stored at -80 °C for later processing. To determine the effect of the TM6B balancer on *Wolbachia*
232 titer, we crossed *Wolbachia*-infected, Act5C-Gal4 driver females to *Wolbachia*-uninfected UAS-
233 anti-Ppyr\LUC males (RRID:BDSC_31603: y^1 v^1; P{$y^{+t7.7}$ $v^{+t1.8}$=TRiP.JF01355}attP2). Unmated,
234 F1 female progeny were sorted and stored as described for the nucleotide biosynthesis gene

235 knockdowns. To determine spatial differences in *Wolbachia* titer, we dissected ovaries from two-
236 day old *r-l* knockdown and sibling control flies. We separated ovaries from living, anesthetized
237 flies in sterile PBS. Ovaries and carcasses from three flies were pooled for each biological
238 replicate and flash frozen, followed by storage at -80 °C for later processing.
239
240 Real-time quantitative RT-PCR analyses of target gene expression
241 Flies were homogenized in TRIzol reagent (Invitrogen), and total RNA was extracted following
242 manufacturer's instructions. RNA extractions were DNase treated (RQ1 RNase-free DNase, New
243 England Biolabs) according to the manufacturer's instructions. cDNA was synthesized using M-
244 MuLV Reverse Transcriptase (New England Biolabs) with random hexamer primers (Integrated
245 DNA Technologies). Quantitative RT-PCR reactions were performed with SensiFAST SYBR Hi-
246 ROX kit (Bioline) and gene-specific primers (Supplemental File S2). All samples were run in
247 technical duplicate alongside negative controls on an Applied Bioscience StepOnePlus qPCR
248 machine (Life Technologies). Gene expression was normalized to endogenous 18S rRNA
249 expression using the Livak method (52).
250
251 Real-time quantitative PCR analyses of *Wolbachia* titer
252 DNA was extracted from individual flies using the Quick-DNA/RNA Pathogen Miniprep kit (Zymo
253 Research) according to the manufacturer's protocol. *ftsZ* primers were used to quantify *Wolbachia*
254 genome copy numbers, which were normalized to host genome copies via 18S quantification
255 using the Livak method (52). Reactions were performed with SensiFAST SYBR Hi-ROX kit
256 (Bioline), and all samples and negative controls were run in technical duplicate on an Applied
257 Bioscience StepOnePlus qPCR machine (Life Technologies).
258
259
260

261 Metabolomics

262 We reared L2 larvae of both wild-type (DGRP-320) and w^{145} flies, with and without *Wolbachia*, on
263 100% and 25% BDSC media for metabolomics analyses. Larvae were collected and processed
264 for metabolomics following published protocols and best practices (53, 54). For each of the eight
265 conditions (genotype**Wolbachia**media), a minimum of six vials were initiated by allowing five
266 pairs of adult flies in each vial to mate and lay eggs for 8 hours. After this period, the adults were
267 removed, and larvae were maintained under standard rearing conditions. Flies were allowed to
268 develop until the L2 stage, at which larvae were stage-verified, picked from the media with a
269 dissecting pin, and transferred to a microcentrifuge tube containing sterile ice-cold 0.9% sodium
270 chloride (NaCl). Approximately 30 larvae originating from the same vial of media were collected
271 and pooled into a single replicate, resulting in a minimum of six independent biological replicates
272 per condition. Larvae were rinsed in 0.9% ice cold NaCl three times, gently pelleted, the liquid
273 was removed, and then the pool of larvae was immediately flash frozen in liquid nitrogen prior to
274 storing at -80 °C for later processing. All pools were processed in under 20 minutes to limit decay
275 of metabolites. For metabolite extraction, samples were first transferred to tared 2 mL screwcap
276 tubes containing 1.4 mm ceramic beads pre-chilled in liquid nitrogen. The sample mass was
277 recorded, and tubes were immediately placed back in liquid nitrogen. 800 mL of prechilled (-20
278 °C) 90% methanol containing 2 µg/mL succinic-d4 acid was added to each sample tube and the
279 sample was homogenized in an Omni Beadruptor 24 for 30 seconds at 6.4 m/s. The samples
280 were removed from the homogenizer, incubated at -20ºC for 1 hr, and centrifuged at 20,000 x g
281 for 5 min at 4 ºC. 600 µl of the supernatant was transferred into a new 1.5 mL microcentrifuge
282 tube and dried overnight in a vacuum centrifuge. Ultra High-Pressure Liquid Chromatography -
283 Mass Spectrometry (UHPLC-MS)-based Metabolomics analyses were performed at the
284 University of Colorado Anschutz Medical Campus, as previously described (55). Briefly, the
285 analytical platform employs a Vanquish UHPLC system (Thermo Fisher Scientific, San Jose, CA,
286 USA) coupled online to a Q Exactive mass spectrometer (Thermo Fisher Scientific, San Jose,

287 CA, USA). The (semi)polar extracts were resolved over a Kinetex C18 column, 2.1 x 150 mm, 1.7
288 µm particle size (Phenomenex, Torrance, CA, USA) equipped with a guard column
289 (SecurityGuard™ Ultracartridge – UHPLC C18 for 2.1 mm ID Columns – AJO-8782 –
290 Phenomenex, Torrance, CA, USA) using an aqueous phase (A) of water and 0.1% formic acid
291 and a mobile phase (B) of acetonitrile and 0.1% formic acid for positive ion polarity mode, and an
292 aqueous phase (A) of water:acetonitrile (95:5) with 1 mM ammonium acetate and a mobile phase
293 (B) of acetonitrile:water (95:5) with 1 mM ammonium acetate for negative ion polarity mode. The
294 Q Exactive mass spectrometer (Thermo Fisher Scientific, San Jose, CA, USA) was operated
295 independently in positive or negative ion mode, scanning in Full MS mode (2 µscans) from 60 to
296 900 m/z at 70,000 resolution, with 4 kV spray voltage, 45 sheath gas, 15 auxiliary gas. Calibration
297 was performed prior to analysis using the Pierce™ Positive and Negative Ion Calibration Solutions
298 (Thermo Fisher Scientific). Acquired data was converted from raw to mzXML file format using
299 Mass Matrix (Cleveland, OH, USA). Samples were analyzed in randomized order with a technical
300 mixture injected after every 24 samples to qualify instrument performance. Metabolite
301 assignments were performed using accurate intact mass (sub-10 ppm), isotopologue
302 distributions, and retention time/spectral comparison to an in-house standard compound library
303 (MSMLS, IROA Technologies, NJ, USA) using El-MAVEN (Elucidata, San Francisco, CA, USA).
304

305 Statistics and Data Visualization

306 Statistics and data visualization were carried out in R version 3.5.0 (31). Significant differences in
307 development were assessed with generalized linear mixed-effects models (package: 'lme4',
308 function 'glmer' (56)) including the proportion of flies that reached a given stage (pupa or adult)
309 as a binomial response, *Wolbachia* presence, day of development, media, and the interaction of
310 the three as fixed effects, and vial as a random effect to account for repeated measures.
311 Significant differences in pupal volume of flies reared on 12.5% media was assessed with a two-
312 way ANOVA (function 'aov') including *Wolbachia*, mortality status, and their interaction as fixed

313 effects. Significant differences in sizes of pupae reared on supplemented media was first
314 assessed with a two-way ANOVA (function 'aov') including *Wolbachia*, media, and their interaction
315 as fixed effects. Paired comparisons between *Wolbachia*-infected and uninfected flies were then
316 assessed with Wilcoxon rank sum tests (function 'wilcox.test'). Gene expression and *Wolbachia*
317 titers from knockdown experiments were assessed with two-way ANOVAs (function 'aov')
318 including delta delta Ct as the response, and target locus, genotype (knockdown versus sibling),
319 and their interaction as fixed effects. *Wolbachia* titers in dissected flies were also assessed with
320 ANOVA, here with genotype, tissue, and their interaction as fixed effects. Pairwise comparisons
321 were performed with t-tests. Similarity of metabolomics samples were visualized with non-metric
322 multidimensional scaling (NMDS) using the 'metaMDS' function from the R 'vegan' package (57)
323 and euclidean distances. Sample collection and data processing for the DGRP-320 and w^{145} flies
324 were carried out on separate dates so genotypes were analyzed separately. Differential
325 abundance of metabolites was determined with MetaboAnalyst 6.0 (58) and leveraged
326 normalization by sample mass, square root transformation, and pareto scaling followed by default
327 analysis parameters.
328

329 **RESULTS**

330 <u>*Wolbachia* infection drastically alters larval gene expression</u>

331 Given that the *Wolbachia*-host relationship is relatively unexplored in juvenile insects, we used a
332 transcriptomics approach to broadly investigate the differences in larval biology when flies are
333 infected with *Wolbachia*. At the second instar (L2) stage, 1,477 genes (~14% of all expressed
334 genes) were significantly differentially expressed ("DEGs") between the *Wolbachia* infected and
335 uninfected flies (786 upregulated; 691 downregulated in the presence of *Wolbachia*; see
336 Supplemental Table S4). DEGs had as much as ~100-fold change in expression. Included in the
337 set of DEGs were two critical regulators of development, both downregulated in the presence of
338 *Wolbachia*: *notch* and the insulin receptor *InR.* Additional related DEGs included *Ist* (a peptide

339 hormone that suppresses insulin production, upregulated), *apolipophorin* (downregulated), *smr*
340 (mediates repression of ecdysone and Notch signaling, downregulated), *ecdysis triggering*
341 *hormone* and its receptor (*eth* and *ethr*, both upregulated), and the juvenile hormone (JH) receptor
342 *met* (upregulated), plus a suite of JH binding proteins (*jhbp4*, -11, -12, and -16, all upregulated
343 except for *jhbp11*).
344
345 Many proteins involved in mitochondrial biology were also significantly differentially expressed
346 (Figure 1). These included several mitochondrial ATP synthases (all downregulated),
347 mitochondrial replication, transcription, and translation related proteins (e.g., mtDNA-helicase,
348 MTPAP, mEFG1, mRpS10, LeuRS-m; all upregulated), heat shock proteins, transporters, and a
349 suite of other enzymes involved in various aspects of mitochondrial metabolism (e.g., NADH
350 dehydrogenase ND-20L, AIF, Gpo1, Sardh, mt:ND6, Acly, Taz, Tpi, amongst others). Importantly,
351 the DEGs included several genes encoding components of the electron transport chain (Cyt-c-d,
352 COX4L, COX5BL, COX7AL; all between 9- to 12-fold downregulated in *Wolbachia* infected
353 larvae). Perhaps functionally related to the impacts on mitochondrial physiology, glutathione
354 metabolism was largely upregulated in the *Wolbachia* infected flies (e.g., *gss1*, *gss2*, *gstE6*,
355 *gstE9*, *gclm*, *gclc*, *gclm*), consistent with a number of previous reports that *Wolbachia* alters redox
356 balance (13).
357
358 Notably, we also identified significant impacts of *Wolbachia* infection on the Toll and IMD immune
359 pathways in the presence of *Wolbachia*. This includes downregulation of the Toll activator *spatzle*
360 and its processing enzyme (SPE); downregulation of antimicrobial proteins including *attacins* (A,
361 B, and D), *defensin*, and *baramicin-A1*; and differential expression of two pattern recognition
362 receptors: peptidoglycan recognition proteins *pgrp-sa* (downregulated) and *pgrp-lb* (upregulated).
363 We also saw a significant overrepresentation of unnamed genes: 36% of all the expressed genes

364 were unnamed (e.g., only have the CG designation), whereas 47% of the DEGs were unnamed
365 (X-squared = 69.12, df = 1, $p < 0.0001$).
366
367 To provide a more holistic look at the list of DEGs, we used two approaches: (1) over-
368 representation analyses, and (2) network visualization based on protein-protein interactions. The
369 DEGs were significantly overrepresented for 29 different gene sets including 13 KEGG pathways,
370 8 molecular functions, 4 preferred tissues, 2 biological processes (cuticle and molting), and 2
371 cellular components (both extracellular) (Supplemental Table S5, Figure 1A). Many
372 overrepresented KEGG pathways have connections to mitochondrial biology and carbohydrate
373 metabolism (e.g., glutathione biosynthesis/metabolism, glycolysis, gluconeogenesis, carbon
374 metabolism, glycan degradation). Additionally, overrepresented KEGG pathways include vitamin
375 B6 metabolism, de novo purine biosynthesis, adenine degradation, and tryptophan metabolism.
376 Other overrepresented gene sets largely point towards digestion and nutrient storage. For
377 example, preferred tissues included the digestive system, fat body (the primary site of fat storage),
378 and muscle (the primary site of carbohydrate storage), and many overrepresented molecular
379 functions were enzymatic (e.g., hydrolases, peptidases, lipases).
380
381 Given these signatures of altered mitochondrial biology, we specifically extracted mitochondrial
382 processes from the DEG set and assessed expression across different functions (Figure 1B). A
383 wide range of mitochondrial processes were represented in the DEG set. The most abundant
384 DEGs, both in absolute number and degree of over-representation, were those related to
385 oxidative phosphorylation: largely downregulated. Energy generation processes such as
386 glycolysis and the tricarboxylic acid (TCA) cycle were similarly overrepresented and also largely
387 downregulated. In contrast, transport-related functions (e.g., transmembrane transport and
388 carriers) and core mitochondrial processes such as translation, transcription and replication,
389 amino acid and protein metabolism, and mitochondrial dynamics were primarily upregulated.

390 These data point to two contrasting impacts of *Wolbachia* infection on mitochondrial function: an
391 up regulation of core processes but a down regulation of carbon and energy metabolism.
392
393 Network analyses revealed that 418 of the DEGs (28.3%) form two high confidence networks
394 (Figure 1C, Supplemental Figure S1), each of which was also associated with significantly
395 overrepresented STRING clusters (Supplemental Table S6). Because the list is long and
396 somewhat redundant due to the nested nature of functional annotations, we summarize the
397 findings as they relate to Figure 1C below. The larger network contains three clusters, each with
398 proteins corresponding to different significantly overrepresented functional categories (Figure 1C,
399 1-3). The "C-1" cluster is strongly downregulated in *Wolbachia*-infected flies and contains many
400 of the aforementioned unnamed genes. While unnamed, many of these proteins are predicted
401 peptidases. DEGs were significantly overrepresented for terms related to transmembrane
402 transport and protein localization to microtubule, and the related genes are also largely clustered
403 in "C-1". The "C-2" cluster is primarily upregulated in the presence of *Wolbachia*. Significantly
404 overrepresented terms that cluster in C-2 include signal, serine proteases (e.g. the Jonah
405 proteases, "Jon*"), extracellular, hydrolase, digestion, carboxypeptidase, and transmembrane
406 transport *). The "C-3" cluster is also upregulated in the presence of *Wolbachia*. Significantly
407 overrepresented terms here are related to translation, specifically ribosome biogenesis and tRNA
408 modification. While not significantly overrepresented, there were many DEGs related to purine
409 nucleotide metabolism: these can be seen below cluster C-3 and include genes such as *prat*,
410 *prat2*, and *ade3*. Finally, the second, smaller network (Figure 2C-4) is strongly upregulated in the
411 presence of *Wolbachia* and made up of proteins that correspond to the significantly
412 overrepresented terms signal, cuticle development, and chitin. Interestingly, this network also
413 includes *ipod*, the interacting partner of Dnmt2 (an RNA methyltransferase previously implicated
414 in *Wolbachia*-mediated pathogen blocking (59)).

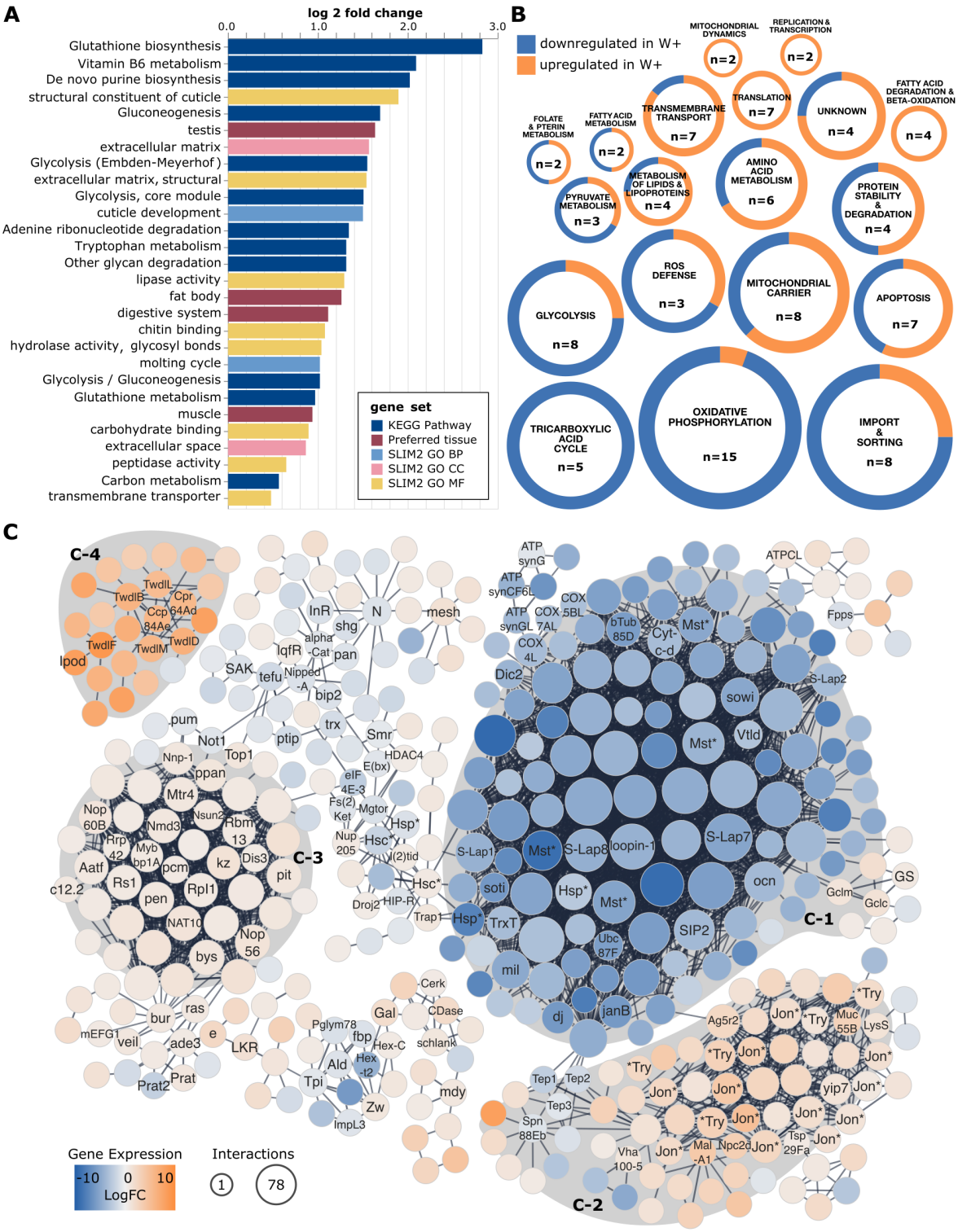

Figure 1. *Wolbachia* infection is associated with differential expression of 14% of the larval transcriptome. (A) Significantly enriched gene sets within the DEGs were assessed for enrichment using PANGEA (37). Log2 fold change values indicate the amount of enrichment for

419 a given gene set, and color coding corresponds to the database of origin for a given gene set.
420 Gene Ontology (GO) gene sets are the *Drosophila* GO Subsets (GO slim) for Biological Process
421 (BP), Cellular Component (CC), and Molecular Function (MF). **(B)** Mitochondrial related DEGs.
422 Each circle represents a functional group, as defined by mitoXplorer, with colored slices indicating
423 the proportion of genes in that group that were up- or down-regulated in response to *Wolbachia*
424 infection. The values "n=" in each circle indicate the number of DEGs in that group, and the size
425 of the circle is a relative indicator of the level of overrepresentation as compared to genomic
426 background. **(C)** Core protein-protein interaction networks within the differentially expressed gene
427 set. Nodes (proteins) are colored according to their change in gene expression relative to
428 uninfected larvae. The size of each node corresponds to the number of interactions that protein
429 has with others in the network. Nodes are labeled if the gene has a name, and either (1) has
430 greater than two connections, or, (2) if the gene was discussed elsewhere in the main text. Some
431 gene names are abbreviated using an asterisk to denote variations on the base family gene name.
432 These include Jon* (e.g., Jon99Fii, Jon66Ci, etc), Mst*, Hsp*, Hsc*, *Try (e.g., alphaTry,
433 lambdaTry, etc). The full network with all nodes annotated with their full gene names is available
434 as Supplemental Figure S1. Shaded regions denote clusters of the gene expression network that
435 are significantly overrepresented with the following functional terms: **(C-1)** uncharacterized
436 peptidases, transmembrane transport, protein localization to microtubule, **(C-2)** signal, serine
437 proteases, extracellular, hydrolase, digestion, carboxypeptidase, transmembrane transport, **(C-3)**
438 ribosome biogenesis and tRNA modification, and **(C-4)** signal, cuticle development, chitin. Full
439 details of all categories and statistical tests for the data represented in panels A and B are in
440 Supplemental Tables S5 and 6, respectively.
441
442 <u>Dynamics of *Wolbachia* gene expression and metabolism across fly development</u>
443 Given the striking impact of *Wolbachia* infection on the larval transcriptome, and the historically
444 strong focus on *Wolbachia* biology in adults, we leveraged an existing dataset to better assess

445 (1) how *Wolbachia* might be interacting with juvenile hosts, and, if (2) patterns in *Wolbachia* gene
446 expression might be functionally relevant to the changes we saw in larval gene expression. We
447 identified several key features of *Wolbachia* gene expression across host development (Figure
448 2A): (1) there is a major shift in global *Wolbachia* gene expression that coincides with the transition
449 to pupation (the transition between third instars (L3) and white pre-pupae (WPP)), (2) distinct
450 clusters of genes have relatively high or low expression pre- and post- pupation, and, (3) genes
451 with different evolutionary histories (e.g., core *Wolbachia* proteins, *w*Mel-specific genes) were
452 non-randomly distributed across the expression clusters (Figure 2B; X-squared = 205.97, df = 25,
453 $p < 0.0001$). For example, genes in cluster 1 were more highly expressed pre-pupation (Figure
454 2A), and significantly more likely to be a core *Wolbachia* gene (Figure 2B). In contrast, cluster 3
455 genes followed an opposite pattern: low expression pre-pupation and high expression post
456 pupation. Additionally, the clustering algorithm identified two sub-clusters within cluster 3, and
457 these largely correspond to genes that have high expression in pupae versus those with high
458 expression in adult males. Cluster 3 was significantly overrepresented for transposition-related
459 genes (Supplemental Table S9), and largely contained IS4/5 family transposases. In contrast,
460 cluster 1 was significantly enriched for many GO terms related to core metabolism (Supplemental
461 Table S8, Figure 2C). The strong upregulation of *Wolbachia*'s metabolic pathways in juvenile flies
462 likely relates to *Wolbachia*'s own metabolic needs. However, this pattern might also be part of a
463 regulatory strategy to limit negative impacts on the host and/or shift roles to better interface with
464 different aspects of host biology across development. Regardless, the up regulation of *Wolbachia*
465 metabolism in juveniles likely plays an important role in shifting the fly metabolic landscape.
466 Finally, it is notable that the most evolutionarily conserved *Wolbachia* proteins are more highly
467 expressed in juveniles, perhaps pointing more broadly towards the importance of these stages
468 across other *Wolbachia*-host associations.

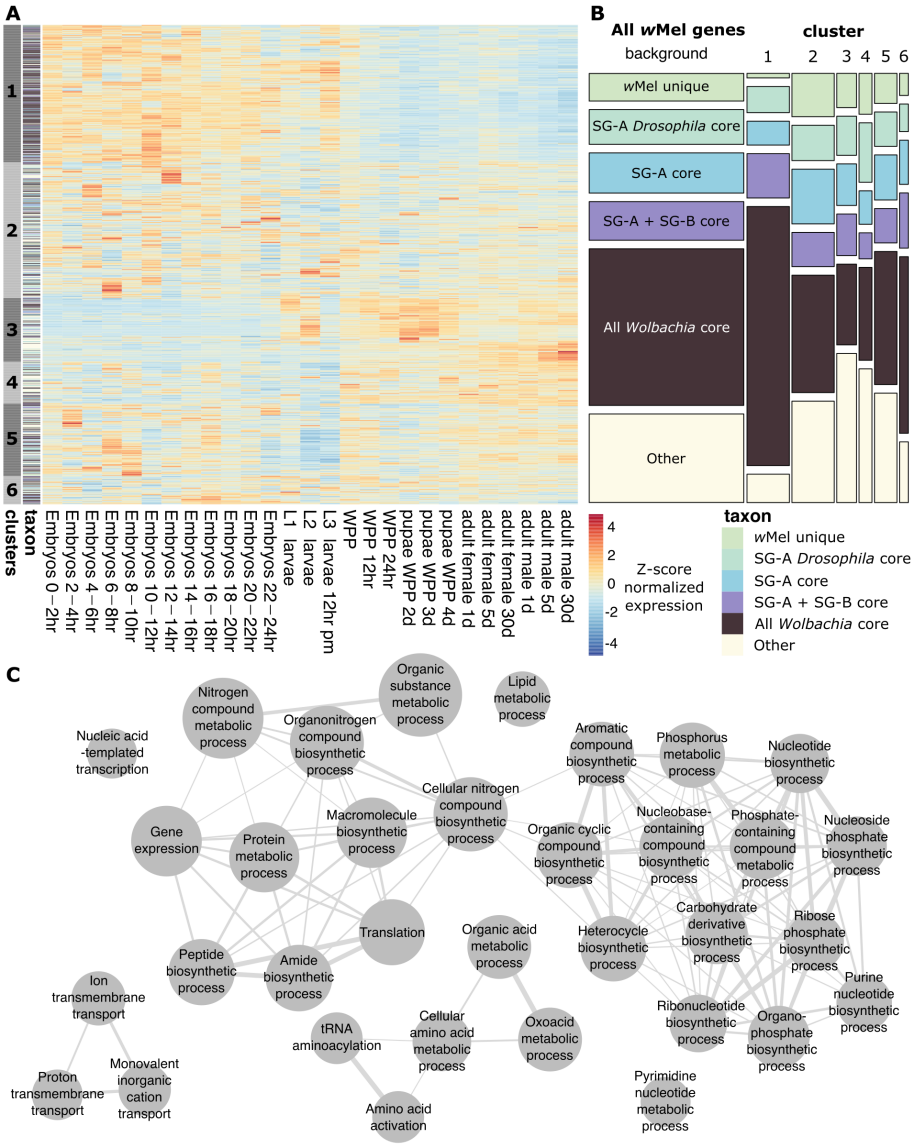

Figure 2. Global *Wolbachia* gene expression patterns during fly development. (A) Gene expression of all *w*Mel genes across fly development. *Wolbachia* transcriptomes were generated as part of the MODENCODE project (40, 41). Data are row normalized (z-score) and heatmap coloring indicates the relative expression of a given gene. Genes were clustered according to similarity of expression patterns across development, and each gene was assigned a taxonomic rank based on conservation relative to other *Wolbachia*. Taxonomic rank assignments include the following categories: (1) unique to *w*Mel, (2) core to the *Drosophila*-infecting clade within Supergroup A (*w*Mel, *w*Ri, *w*Au, *w*Rec, *w*Ha, *w*Suz), (3) core to Supergroup A, (4) core to

478 Supergroups A and B, (5) core proteins across all *Wolbachia*, and, (6) all other *w*Mel proteins. **(B)**
479 Mosaic plot showing the relative proportion of *w*Mel genes within a cluster at each taxonomic
480 rank, relative to all expressed *w*Mel genes ("background"). Abbreviations: Supergroup (SG), white
481 prepupae (WPP), larval instars 1, 2, and 3 (L1, L2, L3), 12 hours pre-metamorphosis (12 hr pm).
482 **(C)** Network of significantly overrepresented GO terms (nodes) derived from cluster 1 genes.
483 Edges indicate at least 20% shared genes, with thicker edges indicating more shared genes.
484

485 <u>*Wolbachia* is beneficial under nutrient limited conditions</u>

486 Given the strong impact of *Wolbachia* on larval gene expression and the differential regulation of
487 *Wolbachia* metabolic gene expression across fly development, we hypothesized that *Wolbachia*
488 would impact fly developmental trajectories. To test this, we reared flies on 100% strength and
489 25% strength media and quantified pupation and adult emergence. We found a significant
490 interaction between *Wolbachia*, media strength, and time that impacted fly pupation ($F_{1,1063}$ =
491 24.7147, $p < 0.0001$) and adult emergence ($F_{1,1063}$ = 22.2897, $p < 0.0001$). Additionally, we found
492 a significant interaction between the presence of *Wolbachia* and the media strength (wild-type
493 pupae: $F_{1,1063}$ = 0.6517, p = 0.0063; wild-type adults: $F_{1,1063}$ = 0.1746, p = 0.0062; w^{145} pupae: $F_{1,711}$
494 = 8.8129, p = 0.0009; w^{145} adults: $F_{1,711}$ = 19.0998, $p < 0.0001$), along with a significant impact of
495 *Wolbachia* infection alone on fly pupation and adult emergence (wild-type pupae: $F_{1,1063}$ = 0.2874,
496 $p < 0.0001$; wild-type adults: $F_{1,1063}$ = 0.5375, $p < 0.0001$; w^{145} pupae: $F_{1,711}$ = 10.5483, $p < 0.0001$;
497 w^{145} adults: $F_{1,711}$ = 7.0718, $p < 0.0001$). For example, while the wild-type flies with and without
498 *Wolbachia* reared on 100% strength media reached adulthood in 82% and 81% of cases, but on
499 the 25% strength media these were reduced to 75% and 66%, respectively. The *Wolbachia*-
500 mediated advantage was more prominent for a second fly genetic background, w^{145}. Even on
501 100% strength media, the *Wolbachia*-free w^{145} flies experienced a 5% reduction in adult
502 emergence relative to *Wolbachia*-infected flies (Figure 1D). When reared on 25% strength media,
503 the *Wolbachia*-infected w^{145} flies were more than twice as likely to reach adulthood (70% versus

504 31%, Figure 1E). Across these assays, we found delays in entering pupation are approximately
505 equal to the delay in adult emergence: *i.e.,* the time spent in metamorphosis did not change as a
506 factor of *Wolbachia* infection. In summary, the *Wolbachia*-mediated advantage is driven by (1)
507 *Wolbachia*-infected flies developing faster (1-5 days depending on genotype, Figures 1B and 1E)
508 and a (2) a larger percentage of flies reaching adulthood.
509
510 Given that the effect size for the *Wolbachia* advantage was genotype dependent and that there
511 was a more subtle impact of *Wolbachia* in the wild-type flies, we wondered if an even weaker
512 media would result in a stronger advantage for the *Wolbachia*-infected flies. Conversely,
513 *Wolbachia* could be a burden under more significant nutritional stress. Indeed, when flies were
514 raised on 12.5% strength media, we again saw significant effects of the interaction between
515 *Wolbachia* and time on the rate and success of pupation and adult emergence (pupae: $F_{1,347}$ =
516 77.135, $p < 0.0001$; adults: $F_{1,347} = 58.9296$, $p < 0.0001$). However, *Wolbachia*-infected flies now
517 developed slower than their uninfected counterparts (6-7 days delayed), but they pupated at
518 higher rates (68% versus 61%) and were more likely to reach adulthood (54% versus 40%, Figure
519 1C). Furthermore, although *Wolbachia*-infected fly development was slower, it resulted in them
520 attaining, on average, a 23% larger size at pupation ($F_{1,191} = 32.076$, $p < 0.0001$, Figure 1F).
521 Additionally, *Wolbachia*-infected flies experienced lower levels of pupal mortality (35% versus
522 19%), perhaps related to the finding that flies that died during pupation were significantly smaller
523 ($F_{1,191} = 4.625$, $p = 0.0328$, Figure 1F).
524
525 To determine if the developmental advantage was due to direct effects of *Wolbachia* or indirect
526 effects via *Wolbachia*-mediated impacts on the gut microbiome, we performed the same
527 developmental assay under axenic conditions (i.e., without a gut or food microbiome). Under
528 axenic conditions, we saw a strong interactive effect of *Wolbachia* and time that resulted in
529 significantly more, and faster, pupation and adult emergence for infected flies (Figure 1G; pupae:

530 $F_{1,1920} = 153.3796$, $p < 0.0001$; adults: $F_{1,1920} = 129.6080$, $p < 0.0001$). Even on the 100% strength
531 media, only 43% of *Wolbachia*-free flies pupated, compared to 61% of *Wolbachia*-infected flies.
532 Again, *Wolbachia*-free flies had higher levels of pupal mortality: 21% of those that pupated did
533 not emerge as adults, as compared to 13% of the *Wolbachia*-infected pupae. While removing the
534 microbiota negatively impacted fly developmental timing as expected, this effect was exacerbated
535 in the *Wolbachia*-free flies (Figures 1A and 1G). As compared to the conventionally-reared flies
536 on 100% strength media (Figure 1A), axenic *Wolbachia*-infected flies experienced a two-day
537 developmental delay, and *Wolbachia*-free flies were delayed three days (Figure 1G). The
538 combination of axenic conditions and 25% strength media resulted in especially impaired fly
539 development: less than 20% of flies reached adulthood (Figure 1H). While there were no
540 significant differences in the proportion of flies that pupated or emerged as adults between
541 *Wolbachia*-infected and uninfected flies in these high-mortality conditions (pupae: $p = 0.9547$;
542 adults: $p = 0.6210$), it is notable that *Wolbachia*-infected flies on average started emerging five
543 days ahead of the *Wolbachia*-free flies (Figure 1H). Finally, we measured the puparia of the axenic
544 flies reared on 100% strength media (Figure 1I) and found that *Wolbachia* infection resulted in,
545 on average, 10% larger pupal volumes ($F_{1,200} = 11.69$, $p = 0.0008$, Figure 1I), again indicating a
546 significant developmental advantage.

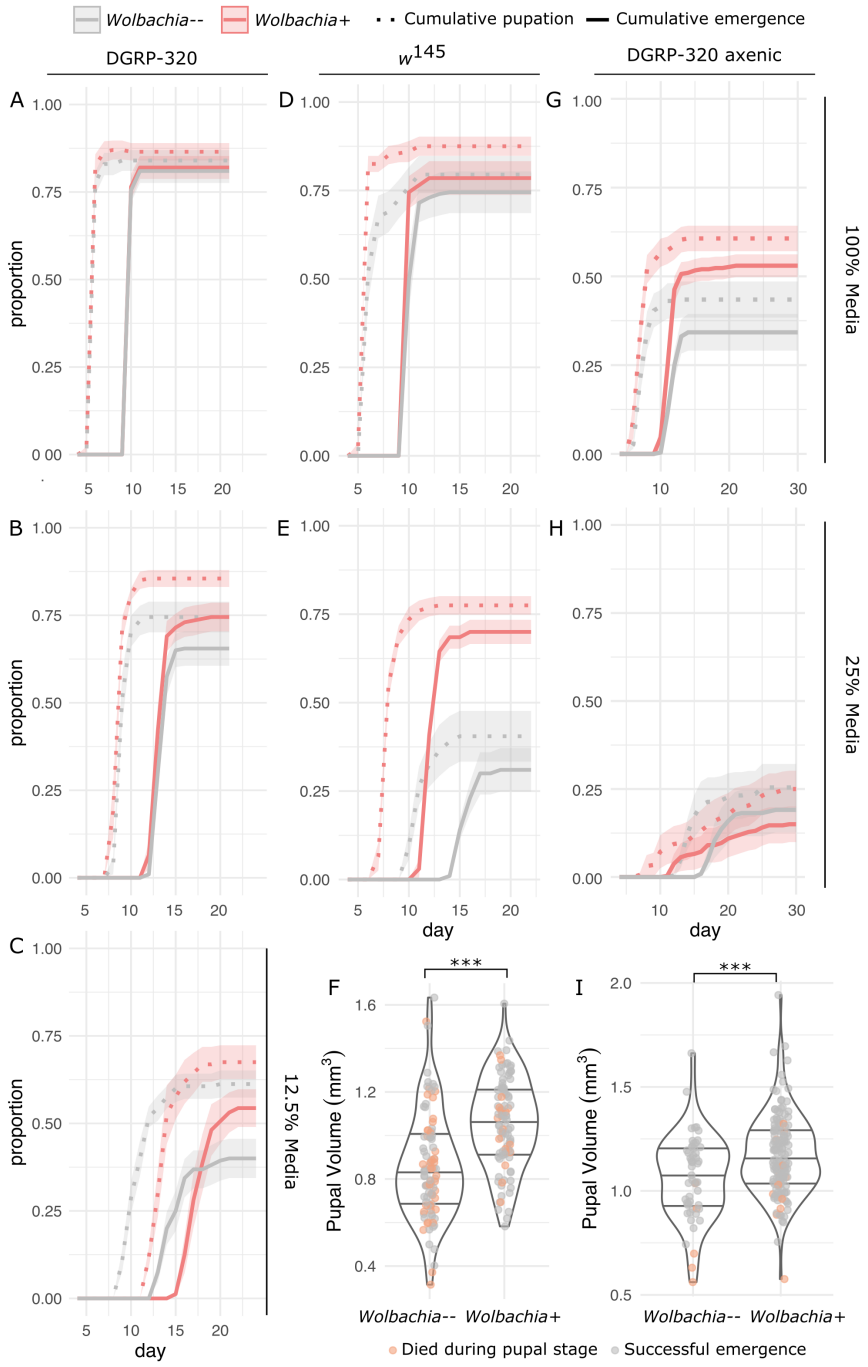

547

548 **Figure 3. *Wolbachia* infection is beneficial under nutrient limited conditions**. Flies (wild-type
549 DGRP-320 and w^{145}, with and without *Wolbachia*) were reared on different concentrations of
550 media to test the impact of *Wolbachia* infection. Biological replicates included 20 larvae per each
551 of 10 vials. Dotted and solid lines indicate cumulative pupation and adult emergence, respectively,
552 with shaded regions defining standard error. All *Wolbachia*-infected treatments are in red, and

553 *Wolbachia*-uninfected in grey. **(A)** Conventionally reared wild-type flies on 100%, **(B)** 25%, and
554 **(C)** 12.5% strength media. **(D)** Conventionally reared w^{145} flies on 100% and **(E)** 25% strength
555 media. **(F)** Pupal volumes of wild-type flies with and without *Wolbachia*, derived from the 12.5%
556 media-reared flies in (C). **(G)** Axenic wild-type flies on 100% and **(H)** 25% strength media. **(I)**
557 Pupal volumes of the axenic-reared flies on 100% strength media derived from (G). Orange
558 datapoints (H-I) indicate pupae that did not eclose into adults. *** $p < 0.001$
559
560 <u>Pyrimidines contribute to the *Wolbachia* infection advantage</u>
561 We reasoned that deficiencies in the diet supplemented by *Wolbachia* could be supplemented by
562 exogenous nutrient addition to the fly food. Therefore, flies with and without *Wolbachia* would
563 have the same growth parameters if this important nutrient was added. Specifically, we focused
564 on the precursors (amino acids) and end-products (uridine and inosine) of *de novo* nucleotide
565 synthesis, because of the related signatures in the fly and *Wolbachia* transcriptomes (Figures 1-
566 2), and our previous data that purines play an important role in the symbiosis (20). We again
567 prepared the 12.5% media which we then supplemented with these compounds. The
568 developmental assays on supplemented media were repeated with the wild-type stocks, avoiding
569 w^{145} because the *white* transporter is known to affect nucleotide metabolism (60). We again saw
570 the *Wolbachia*-mediated developmental advantage in the 12.5% strength media (pupae: $F_{1,235}$ =
571 13.9505, $p = 0.0002$; adults: $F_{1,235} = 12.7568$, $p = 0.0004$). Additionally, we saw a subtle but
572 significant positive impact of *Wolbachia* in the 100% strength media as measured by adult
573 emergence (pupae: $F_{1,235} = 1.3002$, $p = 0.2538$; adults: $F_{1,235} = 28.0455$, $p < 0.0001$), due to 6%
574 pupal mortality in the *Wolbachia*-free flies that the *Wolbachia*-infected flies did not experience
575 (Figure 4A). While the addition of casein benefited both *Wolbachia*-infected and uninfected flies,
576 *Wolbachia*-free flies pupated at significantly increased rates relative to *Wolbachia*-infected flies
577 ($F_{1,235} = 9.8699$, $p = 0.0017$). Again, pupal mortality was quite high in the *Wolbachia*-free flies (36%
578 as compared to 9% with *Wolbachia*), resulting in significantly fewer numbers of adults ($F_{1,235}$ =

579 6.9988, p = 0.0082). The addition of uridine (product of *de novo* pyrimidine synthesis) specifically
580 benefited *Wolbachia*-free flies, but not the flies that had *Wolbachia* infections. Indeed, uridine
581 supplementation resulted in a rescue phenotype where equivalent numbers of *Wolbachia*-infected
582 and uninfected flies emerged as adults (p = 0.9281). Importantly, emergence of *Wolbachia*-free
583 flies supplemented with uridine was not significantly different than the *Wolbachia*-infected flies on
584 the standard 12.5% strength media (p = 0.9097) (Figure 4A). In fact, *Wolbachia*-free flies
585 supplemented with uridine developed slightly faster than their infected counterparts (pupae: $F_{1,235}$
586 = 2.2401, p = 0.1348; adults: $F_{1,235}$ = 10.5842, p = 0.0011). The addition of inosine (product of *de*
587 *novo* purine synthesis) was toxic and reduced pupation and emergence for all flies. As such there
588 were no significant differences between *Wolbachia*-infected and uninfected flies in these high
589 mortality (*i.e.*, zero-inflated) conditions (pupae: $F_{1,235}$ = 0.9217, p = 0.335; adults: $F_{1,235}$ = 0.3519,
590 p = 0.553). Simultaneously adding uridine and inosine resulted in more intermediate, albeit still
591 quite lethal developmental phenotypes with no significant impact of *Wolbachia* ($F_{1,235}$ = 1.3471, p
592 = 0.2459; adults: $F_{1,235}$ = 1.0400, p = 0.307).
593
594 Congruent with the previous developmental assays (Figure 3), *Wolbachia* infection had a
595 significant impact on pupal size, both due to interacting effects with the media ($F_{5,470}$ = 2.55, p =
596 0.0272), and *Wolbachia* alone ($F_{1,470}$ = 37.31, p < 0.0001) (Figure 4B). Furthermore, *Wolbachia*-
597 infected flies were significantly larger when reared on 100% (p = 0.0401), 12.5% (p = 0.0316),
598 and casein-enriched 12.5% media (p < 0.0001). However, the addition of uridine to the 12.5%
599 media resulted in similarly sized flies regardless of *Wolbachia* infection (p = 0.3685). In summary,
600 *Wolbachia*-free flies were rescued to the same size and level of adult emergence as *Wolbachia*-
601 infected counterparts in uridine (i.e., pyrimidine) supplemented media.

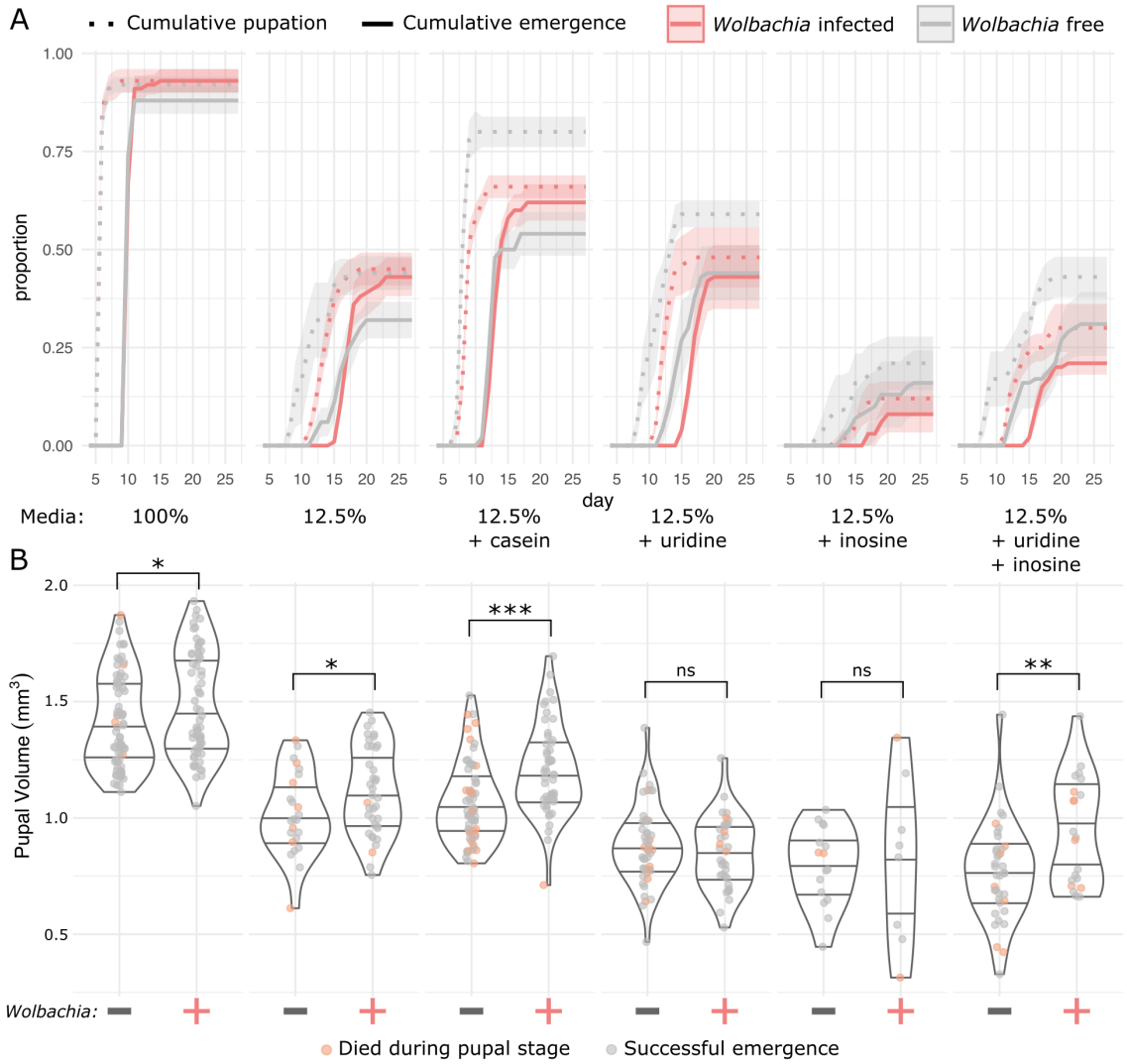

Figure 4. Uridine partially rescues *Wolbachia*-free flies. Wild-type flies were reared on 100% media, 12.5% media, or 12.5% media containing either casein, uridine, inosine, or both inosine and uridine. The media designations in the middle correspond to the figures above and below. Biological replicates included 20 larvae per each of five vials. **(A)** Dotted and solid lines indicate cumulative pupation and adult emergence, respectively, with shaded regions defining standard error. *Wolbachia*-infected treatments are in red and *Wolbachia*-uninfected are in grey. **(B)** Pupae from (A) were removed post-developmental assay, measured, and their volume was calculated. Orange datapoints indicate pupae that did not eclose into adults. Significance annotations for

611 pupal sizes comparisons are the same regardless of whether flies that died during pupation were
612 included. ***$p < 0.001$; **$p < 0.01$; *$p < 0.05$; ns = not significant.
613
614 We were curious about the fact that we also saw a size difference due to *Wolbachia* in the flies
615 reared on 100% media (Figure 4B). Additionally, we noticed that the pupal sizes of the *Wolbachia*-
616 infected flies followed a much more bimodal distribution than did the *Wolbachia* free-flies (Figure
617 4B). We wondered if this was due to differential impacts of *Wolbachia* on male versus female flies.
618 To determine if sex was a contributing factor to the *Wolbachia*-mediated size difference, we
619 measured sex-sorted wild-type pupae, reared on either 100% or 12.5% media, with and without
620 *Wolbachia* (Figure 5). We found significant effects of sex and its interaction with *Wolbachia* or
621 media on pupal size (sex*$Wolbachia$: $F_{1,194} = 9.365$, $p = 0.0025$; sex*media: $F_{1,194} = 17.736$, $p <$
622 0.0001; sex: $F_{1,194} = 265.067$, $p < 0.0001$). As in our previous assay, flies with *Wolbachia* produced
623 significantly larger pupae than those without *Wolbachia* when reared on the 12.5% media ($p <$
624 0.0001). Additionally, this size increase with *Wolbachia* infection was more pronounced in females
625 (41% larger than uninfected pupae) than in males (26% larger). In contrast to our previous assay,
626 there were no significant differences in mean pupal size due to *Wolbachia* for either sex on 100%
627 media (females: $p = 0.9999$; males: $p = 0.8274$). However, in these groups, there were significant
628 differences in the distribution of pupal sizes. Specifically, while uninfected female pupae on 100%
629 media followed a normal distribution (Shapiro-Wilk: $W = 0.9778$, $p = 0.8513$), the infected female
630 pupal sizes significantly deviated from a normal distribution (Shapiro-Wilk: $W = 0.9012$, $p =$
631 0.0228). Similarly, pupal size distributions were significantly different between the *Wolbachia*
632 infected and uninfected males derived from 100% media (Kolmogorov-Smirnov: $D = 0.3896$, p-
633 value = 0.0267).

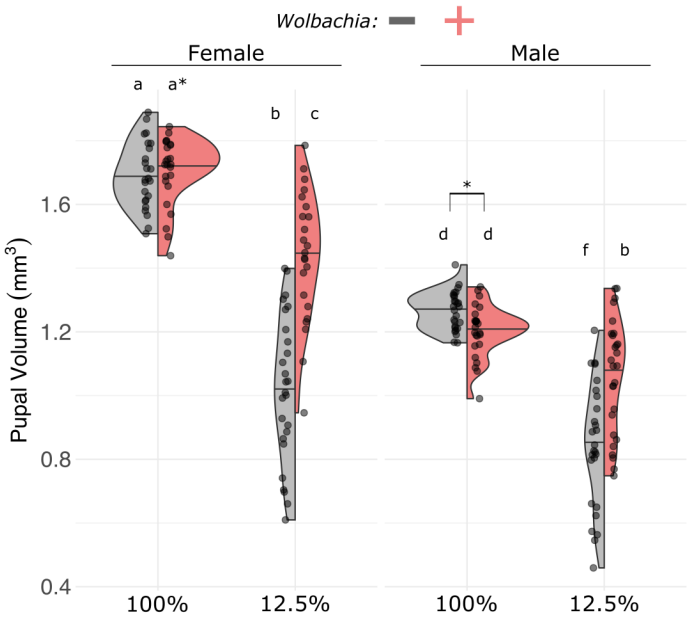

Figure 5. The *Wolbachia* size-advantage is more pronounced for female flies. Wild-type flies were reared on 100% or 12.5% media and collected during pupal stages P13-P14 (51). Pupae were sex sorted, measured, and their volume was calculated. Letters indicate statistically significant differences in mean pupal volume between groups (Tukey's Honest Significant Difference test, $p<0.05$). Asterisks indicate significant differences in distributions.

<u>*Wolbachia* infection is responsive to fly pyrimidine biosynthesis gene expression</u>

To determine whether *Wolbachia* infection was sensitive to changes in host metabolism, we knocked down individual genes within the fly's *de novo* nucleotide synthesis pathways (Figure 6A) using *Wolbachia*-infected RNAi fly stocks (Figure 6B-C). Short-hairpin RNA (shRNA) expression was driven in the entire body of the fly by an Act5C-Gal4 driver. We compared gene expression and *Wolbachia* titer in knockdown flies to sibling controls (flies not expressing a gene-targeting shRNA, and instead with the TM6B balancer). We successfully knocked down four genes in the purine synthesis pathway (*prat2*, *ade2*, *ade5*, *CG11089*) and three genes in the pyrimidine synthesis pathway (*su(r)*, *Dhod*, *rudimentary-like*)(Figure 6B-C). Several gene knockdowns were lethal to fly development, including *rudimentary* in the de novo pyrimidine

651 biosynthesis pathway and *CG2246*, *CG6767*, *Prat*, and *AdSL* in the de novo purine biosynthesis
652 pathway. Broad-spectrum knockdown of *de novo* purine synthesis had no significant impacts on
653 *Wolbachia* titer (gene*knockdown: $F_{3,31}$ = 0.652, p = 0.588; gene: $F_{3,31}$ = 0.644, p = 0.593;
654 knockdown: $F_{1,31}$ = 0.593, p = 0.447; Figure 6D). In contrast, knockdown of the *de novo* pyrimidine
655 synthesis pathway resulted in significant increases in *Wolbachia* titer ($F_{1,38}$ = 10.3916, p = 0.0026;
656 Figure 6E). This pattern was specifically driven by the enzymatic loci (*Dhod*: p = 0.034 and
657 *rudimentary-like* (*r-l*)*:* p = 0.013). In contrast, knockdown of the negative regulator *sur(r)* had no
658 effect on *Wolbachia* titer (p = 0.530), perhaps indicating that *Wolbachia* titers are responsive to
659 low fly pyrimidine synthesis activity, but not elevated levels. To account for any effects of the TM6B
660 balancer on measurements of *Wolbachia* abundance, we crossed the Act5C-Gal4 driver to a RNAi
661 line expressing shRNA against a foreign gene: *Photinus pyralis* luciferase (UAS-anti-Ppyr\LUC).
662 We found no significant changes in *Wolbachia* titer, or in nucleotide gene expression that could
663 be driving the results in Figure 6B (Supplemental Figure S3). We then asked if the change in
664 *Wolbachia* titer was tissue-specific by measuring the relative *Wolbachia* titers in ovaries and the
665 remaining carcasses after knockdown of *r-l* (Figure 6F). There was no significant interaction of
666 knockdown and tissue ($F_{1,32}$ = 0.20, p = 0.658) or of tissue alone ($F_{1,32}$ = 0.20, p = 0.658) on
667 *Wolbachia* titers. We again saw a significant effect of *r-l* knockdown on *Wolbachia* titers ($F_{1,32}$ =
668 13.07, p = 0.001) both in ovaries (p = 0.007) and in carcasses (p = 0.0127) (Figure 6F).

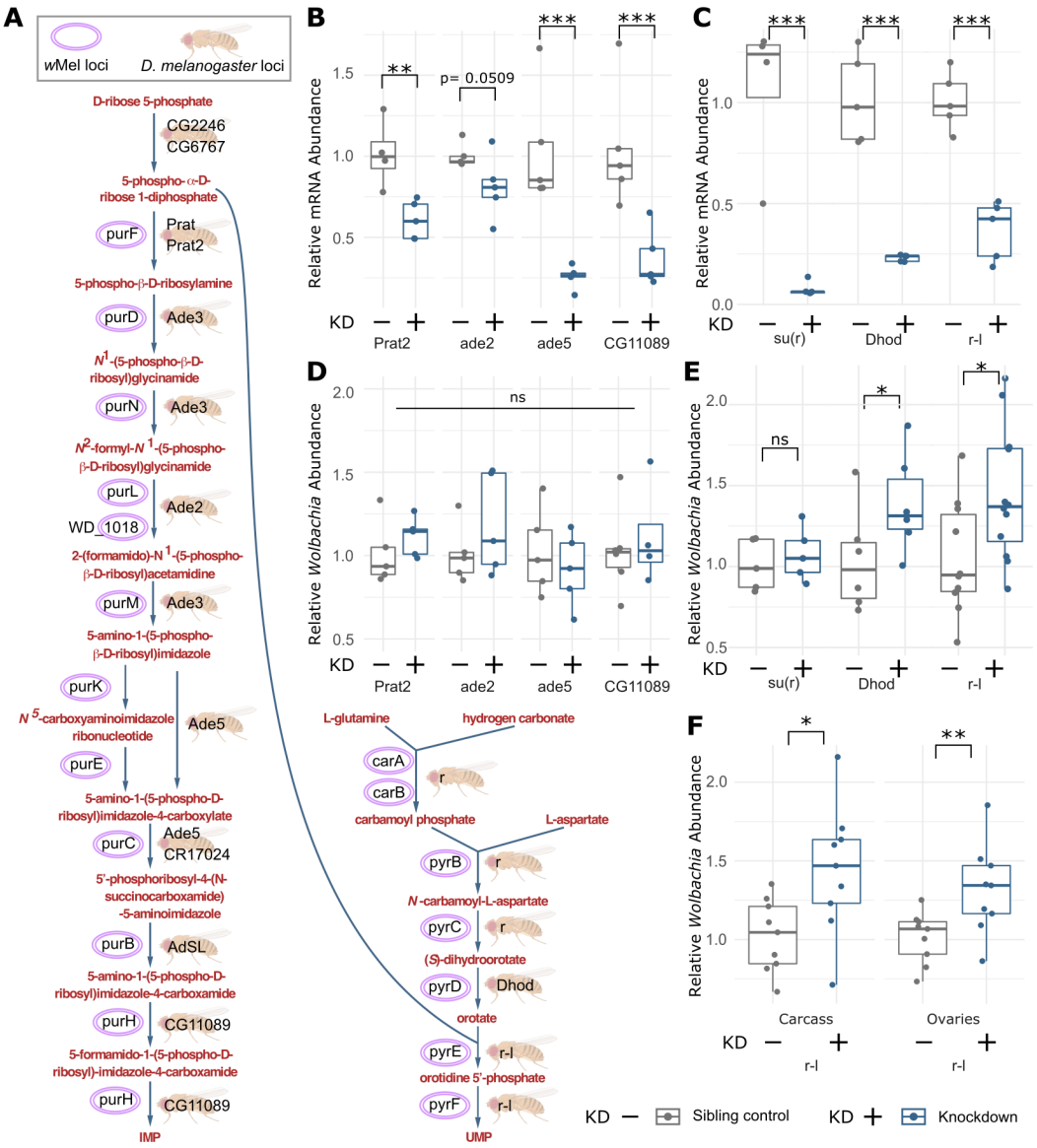

Figure 6. *Wolbachia* titers are responsive to fly pyrimidine synthesis gene expression. (A) Metabolic pathway for *de novo* nucleotide biosynthesis (purine: IMP, left; pyrimidine: UMP, right) in *Wolbachia* and *Drosophila melanogaster.* **(B)** Knockdown of fly purine biosynthetic genes was verified with qRT-PCR leveraging gene specific primers and normalization to 18S expression. **(C)** Knockdown of fly pyrimidine biosynthetic genes was verified with qRT-PCR leveraging gene specific primers and normalization to 18S expression. **(D)** Relative *Wolbachia* titers in whole adult females after purine gene knockdown. **(E)** Relative *Wolbachia* titers in whole adult females after pyrimidine knockdown. **(F)** Relative *Wolbachia* titers in female carcasses and ovaries after

678 constitutive knockdown of *r-l*. In all cases, *Wolbachia* titers were quantified with qPCR using
679 *Wolbachia*-specific primers and normalization to fly genome copy number via 18S amplification.
680 All knockdowns leveraged short-hairpin RNA (shRNA) expression constitutively driven by Act5C-
681 Gal4. Legend: *** $p < 0.001$; ** $p < 0.01$; * $p < 0.05$; ns p = not significant.
682
683 Interactive effects of *Wolbachia*, fly genotype, and diet impact fly metabolism
684 Considering the complex relationship between *Wolbachia* infection and *Drosophila* metabolism,
685 we decided to further examine this relationship using semi-targeted LC-MS-based metabolomics
686 to measure the relative abundance of 259 metabolites in two genetic strains (wild-type DGRP-
687 320 and w^{145}) raised on either 100% or 25% media (Figure 7; Supplemental Tables S10-12). The
688 resulting data revealed that *Wolbachia* induced significant differences in the metabolome of both
689 strains under both dietary conditions (Figure 7A-B). Moreover, the associated changes in the fly
690 metabolome largely correlated with the strength of the developmental phenotype. For example,
691 *Wolbachia* had reduced influence on the metabolome of wild-type flies grown on 100% media
692 when compared with uninfected controls (Figure 7C,E), with only 11 metabolites exhibiting
693 significant difference on the 100% food as compared to the 25 metabolites that were changed on
694 the 25% media. Similarly, the total number of *Wolbachia*-associated metabolites that reached the
695 cutoff threshold for significance in w^{145} was also lower in the 100% media (19 vs 29) (Figure 7D,F).
696
697 Beyond the total number of metabolites that were changed in *Wolbachia*-infected and uninfected
698 larvae, several of the significantly altered compounds function within metabolic pathways that are
699 clearly associated with *Wolbachia* infection. Specifically, in 3 of 4 analyses, *Wolbachia* infections
700 results in reduced levels of the purine degradation products allantoin and allantoate (Figure
701 7C,D,F), whose production is associated with the antioxidant properties of uric acid (61).
702 *Wolbachia* infected w^{145} flies also displayed decreased accumulation of kynurenic acid and
703 cystine – amino acid derived molecules that are involved in the cellular response against oxidative

stress (Figure 7D,F) (62-64). Our analysis also revealed decreases in pantothenate, a precursor to coenzyme A, thus suggesting that *Wolbachia* influences the abundance of a key molecule in mitochondrial metabolism. Finally, we would highlight the interactive impacts on S-adenosyl-L-homocysteine (SAH) abundance in the wild-type flies, an intermediate molecule in glutathione biosynthesis and thus directly involved in the cellular oxidative stress response.

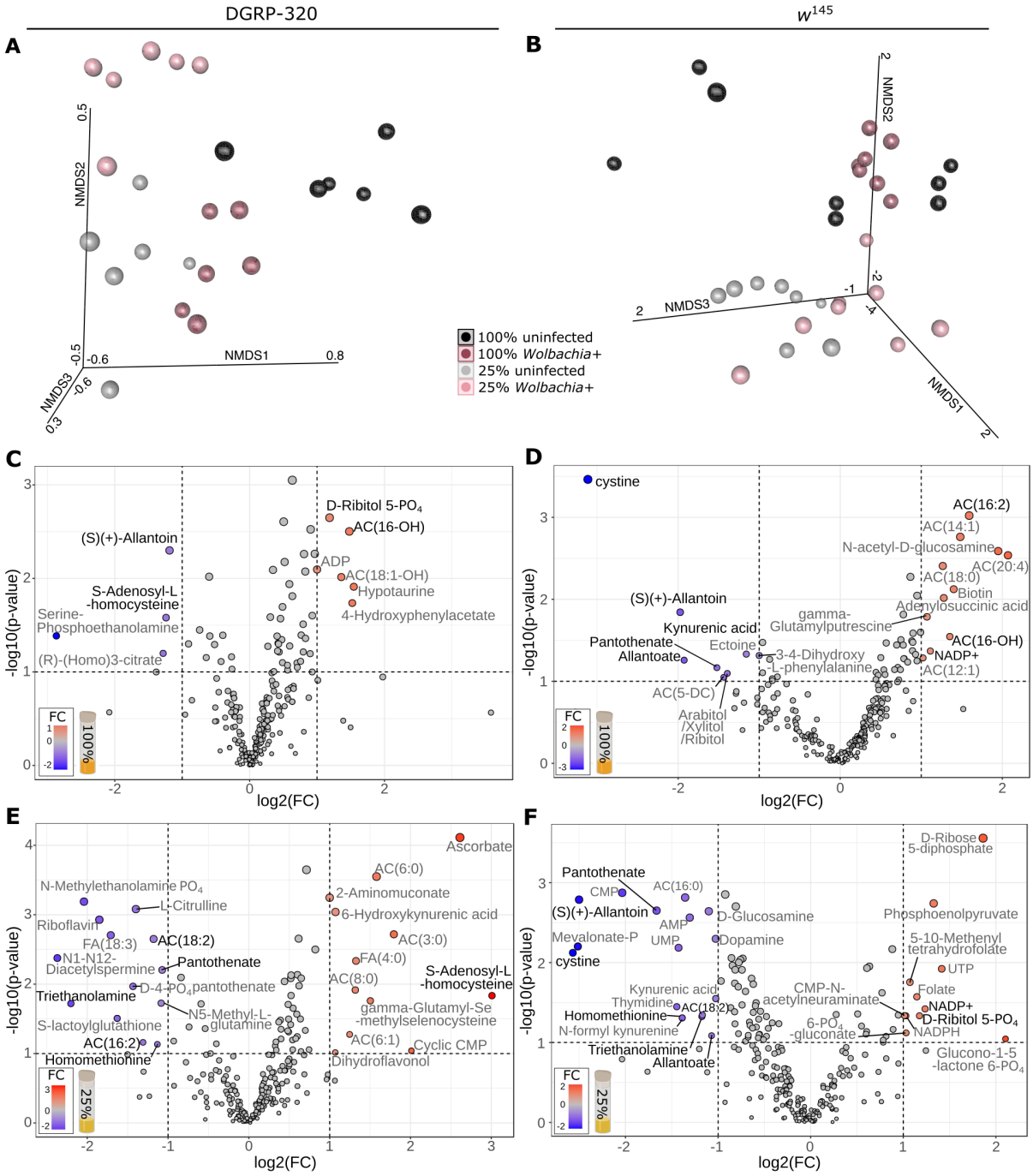

710 **Figure 7. *Wolbachia* mediated impacts on the metabolome depend on host genotype and**
711 **nutrition. (A-B)** Three-dimensional non-metric multidimensional scaling (NMDS) plots indicating
712 relative similarity of (A) DGRP-320 and (B) w^{145} samples. Point size indicates distance from the
713 page, where larger points are closer. **(C-F)** Volcano plots indicating the relative abundance of
714 specific metabolites in *Wolbachia* infected larvae relative to uninfected larvae: **(C)** DGRP-320 L2
715 larvae reared on 100% media. **(D)** w^{145} L2 larvae reared on 100% media. **(E)** DGRP-320 L2 larvae
716 reared on 25% media. **(F)** w^{145} L2 larvae reared on 25% media. Metabolites with >2 $\log_2$ fold
717 change (log2FC) and p<0.1 are indicated, and, for those that met these criteria in >2 conditions
718 (e.g., panels) the metabolite name is in black font rather than grey. "Phosphate" is abbreviated
719 with "PO_4" to save space. "AC(#:#)" or "FA(#:#)" refers to acylcarnitines or fatty acids where
720 numbers in parentheses indicate the total number of carbons in the chain, and the number of
721 unsaturated bonds, respectively.
722
723 **DISCUSSION**
724 *Wolbachia* has long been appreciated for its diverse impacts on a range of ecdysozoan hosts.
725 Increasingly, there is speculation as to the role *Wolbachia* plays in host metabolism more broadly,
726 oftentimes in the context of specific metabolites (12, 20, 21). For example, *Wolbachia*-infection
727 contributes to B-vitamin supplementation in a planthopper (19), bed bugs (15), and likely some
728 species of solitary bees (65). Iron has been the subject of a number of investigations into
729 *Wolbachia*-host interactions (16, 17, 66, 67). In *Drosophila melanogaster, Wolbachia* infection
730 buffers against stresses associated with low or high concentrations of iron in the diet (67).
731 *Wolbachia* infection is additionally associated with changes in host ferritin expression and iron
732 homeostasis in other insects such as *Drosophila simulans* and the parasitoid wasp *Asobara*
733 *tabida* (17). Given the range of metabolites and physiological processes that have been implicated
734 in *Wolbachia*-host interactions, we focused initial experiments on using a more holistic approach
735 to understanding fly development in the context of diet and *Wolbachia* infection.

736

737 Our transcriptomics results contained several surprising findings. First, a huge number of genes
738 were differentially expressed due to *Wolbachia* infection: equivalent to 14% of the transcriptome.
739 This number of DEGs is an order of magnitude larger than the number of DEGs identified in other
740 analyses focused on adult transcriptomes (20). We were also surprised to see a clear impact on
741 expression of the immune system. The prevailing hypothesis in the field has been that natively
742 associated *Wolbachia* (e.g., *w*Mel for *Drosophila melanogaster*) do not trigger an immune
743 response, whereas newly initiated infections (e.g., *w*Mel established in *Aedes* mosquitoes) do
744 trigger an immune response (68). Indeed, while we did not see any induction of the immune
745 system in *Wolbachia*-infected larvae, we did see strong down-regulation of many immunity-
746 associated loci indicating some level of interaction between *Wolbachia* and host in this native
747 association. Other notable findings in the transcriptomes include differential expression of major
748 regulators of metabolism and development such as *Notch*, *InR*, and juvenile hormone signaling
749 related proteins. Genes associated with the digestive system, fat body, muscles, and testes were
750 also significantly more likely to be differentially expressed. While the first three tissues clearly
751 point towards metabolic impacts, we found the pattern of testes-associated genes quite curious
752 given that the analysis focused on L2s which had not been sex sorted. This pattern might reflect
753 sex-specific differences in the timing of gonadal development: ovary morphogenesis does not
754 begin until late L3, whereas testes begin to grow and differentiate substantially during
755 embryogenesis (69). The earlier development of testes likely results in more power to detect
756 *Wolbachia*-mediated impacts in these tissues as compared to in the developing ovaries,
757 especially when using pooled, homogenized, whole animals. However, it is important to note that
758 these metrics of tissue-biased expression are based on the MODENCODE dataset (37, 40, 41),
759 which, as we note above, is derived from *Wolbachia*-infected flies. So, even given these caveats,
760 there is clearly a *Wolbachia*-dependent difference in gene expression across a wide variety of
761 processes.

762

763 Our gene expression data and understanding of *Wolbachia* genome evolution pointed us towards
764 fly development and metabolism as an important regulator of the symbiosis. Indeed, we found
765 that *Wolbachia* significantly impacts *Drosophila melanogaster* development, resulting in larger
766 flies that were more likely to reach adulthood. The strength of this phenotype varied by fly
767 genotype and the overall concentration of nutrition in the food: *Wolbachia* infection was highly
768 beneficial under nutrient limited conditions. Removal of the extracellular microbial community
769 indicated that this advantage was directly mediated by *Wolbachia*. In fact, *Wolbachia* significantly
770 buffered flies against the stresses normally associated with removal of the microbiome (70, 71).
771 Furthermore, *Wolbachia* titers were responsive to changes in the expression of fly pyrimidine
772 synthesis, and the supplementation of pyrimidines rescued adult emergence of the *Wolbachia*-
773 uninfected flies. Importantly, while the transcription of *Wolbachia*'s nucleotide metabolism
774 pathways are quite high pre-pupation (Figure 2), the flies have comparatively low *Wolbachia* titers
775 during that time (40). We propose that pyrimidines are a significant component of the
776 developmental advantage provided by *Wolbachia*. During the ~200-fold increase in larval body
777 mass, there is a concomitant 25-fold increase in DNA and RNA content that creates a huge
778 demand for pyrimidines, well exceeding the fly's endogenous biosynthetic capacity (72).
779 Considering that the rate of *Drosophila* development is highly sensitive to *de novo* pyrimidine
780 synthesis (72), bacterially-derived nucleotides could give the host a significant advantage.

781

782 While we found that pyrimidines seemed to be important for the *Drosophila*-*Wolbachia* symbiosis,
783 we did not see any changes in *Wolbachia* titer due to suppression of purine synthesis (Figure 6),
784 nor did we see purine-mediated rescue of *Wolbachia*-uninfected flies (Figure 4). In fact, the
785 addition of inosine to media negatively impacted flies. While altering the expression of fly purine
786 metabolic gene expression did not impact the relative abundance of *Wolbachia* in our
787 experiments, we cannot rule out the potential for other changes in *Wolbachia* gene expression or

788 physiology. Nevertheless, these patterns are especially curious given that both metabolomics
789 (Figure 7), and larval gene expression data (Figure 1) indicate significantly altered purine
790 metabolism due to *Wolbachia*. And, we previously found an interactive effect of *Wolbachia*
791 infection and the *de novo* purine biosynthesis pathway on virus replication (20), highlighting both
792 the importance of purines to the symbiosis and the complexity of the metabolic landscape. Indeed,
793 purine nucleotides act as signaling molecules that impact a range of functions. For example,
794 activation of the adenosine receptor globally suppresses fly metabolism (73), which can cause
795 insecticidal effects (74). Another possibility to explain the toxic effects of inosine supplementation
796 (Figure 4) is misincorporation of inosine into RNAs. In mammalian cell lines, this can happen
797 when inosine is in excess, ultimately impacting translation (75).
798
799 The contrast between purine and pyrimidine metabolism and their respective roles in the
800 *Wolbachia*-host relationship led us to look more deeply into (1) how these pathways contrast with
801 each other, and (2) how these pathways relate to other metabolic processes in the animal.
802 Pyrimidines are synthesized by a series of metabolic reactions that use ribose sugar and the
803 amino acids glutamine and aspartate to generate uridine-5'-monophosphate, UMP (76): the
804 precursor for uracil, cytosine, and thymine. An enzyme in this pathway, dihydroorotate
805 dehydrogenase (*Dhod*), is located in the inner mitochondrial membrane where it couples
806 pyrimidine synthesis to electron transport (77, 78). This pathway is conserved in both *Drosophila*
807 and *Wolbachia*, suggesting that infected flies generate pyrimidines in multiple compartments: the
808 host cytoplasm/mitochondria and *Wolbachia*. Purine biosynthesis, again conserved between the
809 fly and *Wolbachia*, is a comparatively more complicated pathway that also uses amino acids to
810 build the nucleotide ring (Figure 6A). Additionally, an important early step in this pathway is the
811 production of 5-phospho-α-D-ribose 1-diphosphate (PRPP) which is also used in pyrimidine
812 biosynthesis (Figure 6A). In later steps, the enzyme AdSL generates 5-Aminoimidazole-4-
813 carboxamide ribonucleotide (AICAR, the reactant for the next purine synthesis step, Figure 6A)

814 and fumarate which is transported to the mitochondrion for the citric acid cycle. The connectivity
815 of these two metabolic pathways, their links to amino acid and vitamin metabolism (e.g., folic acid
816 derivatives), and the direct relationship with mitochondria implicates a much more complicated
817 model than *Wolbachia* simply increasing the abundance of a singular limiting metabolite. For
818 example *Wolbachia*-generated pyrimidines could reduce the biosynthetic burden normally
819 imposed upon mitochondria – a model further supported by the ability of UMP to inhibit fly
820 enzymes CAD and UMP synthase, which act as components of the fly's pyrimidine biosynthetic
821 pathway (79). Therefore, *Wolbachia*'s production of pyrimidines could simultaneously impact free
822 amino acid pools (the nucleotide synthesis precursors), reduce mitochondrial burdens, and
823 spatially segregate components of a normally inhibitory interaction.
824
825 Several other metabolites associated with mitochondrial metabolism and redox balance were
826 significantly altered in *Wolbachia* infected animals. Decreases in purine catabolic products,
827 kynurenic acid, cysteine, and SAH highlight metabolic pathways that are clearly associated with
828 *Wolbachia* infection. *Wolbachia*-mediated changes in redox balance have been the subject of a
829 number of previous investigations (80-85), though there are limited functional data to support the
830 ultimate mechanisms responsible. A previously suggested model, based on metabolic differences
831 in adult flies, hypothesized a reprogramming of mitochondrial metabolism, specifically towards
832 non-oxidative metabolism combined with reduced insulin signaling and a hypoxia response (66).
833 Our data largely support this hypothesis, and indeed, we do see downregulation of the insulin
834 receptor and upregulation of a negative regulator in larvae with *Wolbachia*, plus impacts on redox
835 balance. This same model and others (66, 86) further hypothesized that *Wolbachia* is exporting
836 ATP (a purine), which contrasts with our findings that pyrimidines play a key role. However, given
837 the link between these pathways, perhaps our supplementation of the highly limiting pyrimidines
838 resulted in a reduced need for shunting PRPP to the pyrimidine pathway, ultimately allowing
839 greater synthesis of IMP, which can later be converted to ATP. Whether *Wolbachia* are in fact

840 exporting ATP remains to be empirically tested. Importantly, our understanding of *Wolbachia*
841 physiology is largely limited to what we have inferred from genomic data and changes that we
842 can detect in host physiology. While *Wolbachia* encode for an abundance of predicted
843 transporters (3), we do not know if these proteins are functional, if their function agrees with
844 bioinformatic predictions, or if specific metabolites are indeed transported in or out of *Wolbachia*
845 cells.
846
847 Changes in the concentrations of the purine catabolic product SAH specifically point towards a
848 model linking pathogen blocking with potential roles for *Wolbachia* in host metabolism. The
849 observed changes in SAH are also quite intriguing considering that this molecule is both produced
850 by S-adenosyl-L-methionine (SAM) methyltransferases and also inhibits the activity of these same
851 enzymes (87). Since *Wolbachia* is proposed to enhance pathogen blocking by interacting with
852 methylation of viral RNA molecules (88), our results suggest that this phenomenon could be the
853 result of nutrient-dependent influences of *Wolbachia* on the host metabolism. The relative
854 accumulation of SAH could be indicative of higher levels of methyltransferase activity. Notably,
855 the interacting partner (*ipod*) of the fly's methyltransferase (*dnmt2)* was strongly upregulated (68-
856 fold) in the *Wolbachia*-infected larvae. *Wolbachia* may mediate effects on the host's production of
857 SAH, and/or *Wolbachia* might directly produce SAH, as the *Wolbachia* genome encodes for
858 several putative methyltransferases (3). Indeed, our metabolomics approach does not allow us to
859 identify which organism(s) any of the metabolite pools are derived from. However, given the
860 overlap of several key metabolic pathways (Figure 6)(21) we hypothesize that many differences
861 we detect are due to a combination of *Wolbachia*'s own metabolic activity and impacts on the
862 host.
863
864 Our hypothesis that *Wolbachia*'s contributions to metabolism go beyond simple supplementation
865 are further supported by our finding that *Wolbachia* decreases pupal mortality. This was especially

notable during nutritional stress, suggesting that *Wolbachia*-free flies enter pupation despite insufficient metabolic reserves. This effect was most pronounced when flies were reared on an excess of protein (Figure 4). Importantly, amino acids are a key nutritional cue for determining the timing of pupation (i.e., signaling critical weight) due to direct and indirect effects on the timing and intensity of ecdysone pulses (89-92). An influx of amino acids without other essential nutrients needed for growth might impact nutritional signaling and thus the timing of critical weight, perhaps triggering flies to pupate early without sufficient energy stores needed for metamorphosis. *Wolbachia*'s import of amino acids may reduce the concentrations of free amino acids in these protein enriched conditions, which could delay signaling critical weight, allowing flies to accumulate more metabolic reserves before pupation.

The role of *Wolbachia* as a nutritional symbiont raises numerous questions about the cell biology of *Wolbachia* and how the relationship with the host is regulated. Indeed, the patterns of *Wolbachia* gene expression do seem to be attuned to fly development (Figure 2) which could be a strategy for supporting the exponential growth that occurs during larval stages and mitigating fitness impacts of the infection during reproductive stages. Is *Wolbachia* specifically providing pyrimidines or other key metabolites (*e.g.,* via nucleotide transporters)? Or are flies farming and consuming their *Wolbachia* infections (*e.g.,* via autophagy) and pyrimidines so happen to be abundant in *Wolbachia* cells and also a limiting metabolite for the fly? As is the case for many symbioses, it is not always clear if a change in the symbiont (*e.g.,* gene expression or titer), is due to the microbe detecting and responding to the host's status, or the host releasing control of the microbe and "allowing" a change in microbial physiology. *Wolbachia* do encode for a number of proteins that would allow them to detect their environment and regulate gene expression accordingly (93). However, each *Wolbachia* is enclosed by a host-derived vesicle (94, 95), so perhaps the host tightly regulates *Wolbachia*'s "experience". Changes in *Wolbachia* titer and physiology across development and under different nutritional scenarios likely reflect these

892 evolutionary balancing acts, as is evident by the complex manner by which rapamycin feeding
893 and dietary amino acid supplementation influence *Wolbachia* titers (96).
894
895 While beneficial nutritional symbioses in insects are not rare, most of the systems for which this
896 is described are of a much more binary nature. Insects that exclusively feed on unbalanced diets
897 (e.g., blood, plant sap) have obligate microbial symbionts to synthesize metabolites that the host
898 cannot generate *de novo*: the partners complement each other (97, 98). Here, both flies and
899 *Wolbachia* have their own complete pathways for nucleotide biosynthesis, which perhaps has led
900 us to overlook the relevance of this biosynthetic redundancy. Our finding that *Wolbachia*
901 significantly impacts the developmental timing, size, and susceptibility to nutritional stress in a
902 well-studied model such as *Drosophila melanogaster* raises the question of the broader relevance
903 of *Wolbachia* infections to insect metabolism and development.
904
905 **DECLARATIONS**
906 Acknowledgements
907 Research reported in this publication was supported by the National Institute of General Medical
908 Sciences of the National Institutes of Health under award number R35GM150991 and the
909 National Institute of Allergy and Infectious Disease of the National Institutes of Health under award
910 number R21AI175957, both to ARIL. ILGN is supported by the National Institute of Allergy and
911 Infectious Diseases of the National Institutes of Health under R01AI144430. JMT is supported by
912 the National Institute of General Medical Sciences of the National Institutes of Health under
913 R35GM119557. The authors thank Richard Hardy for support and feedback. Research was
914 further made possible by Flybase (NIH 5U41HG000739), and stocks obtained from the
915 Bloomington *Drosophila* Stock Center (NIH P40OD018537).
916
917 Conflicts of interest

The authors declare that they have no competing interests.

Data Availability

Raw RNA-seq data have been deposited in the NCBI Short Read Archive under BioProject PRJNA1111126.

Supplemental Table S1. Fly stocks

Supplemental Table S2. Primers

Supplemental Table S3. Expression data for all expressed genes in the *Drosophila melanogaster* L2 dataset.

Supplemental Table S4. Differentially expressed *Drosophila melanogaster* L2 genes.

Supplemental Table S5. Statistical results for overrepresented gene sets (PANGEA).

Supplemental Table S6. Statistical results for overrepresented terms and clusters (STRING).

Supplemental Table S7. Taxon and cluster assignments for *w*Mel loci.

Supplemental Table S8. *w*Mel cluster 1 statistical results for overrepresented biological process GO terms.

Supplemental Table S9. *w*Mel cluster 3 statistical results for overrepresented biological process GO terms.

Supplemental Table S10. Metabolomics metadata

Supplemental Table S11. DGRP-320 metabolite abundance data

Supplemental Table S12. *w*145 metabolite abundance data

Supplemental Figure S1. Full sized, all-labeled version of RNA-seq network (main text Figure 1C).

Supplemental Figure S2. Pupal measurement.

Supplemental Figure S3. Knockdown controls.

REFERENCES

943 1. R. Kaur *et al.*, Living in the endosymbiotic world of *Wolbachia*: A centennial review. *Cell*
944 *Host & Microbe* **29(6)**, 879-893 (2021).
945 2. O. Duron *et al.*, The diversity of reproductive parasites among arthropods: *Wolbachia* do
946 not walk alone. *BMC Biol.* **6**, 1-12 (2008).
947 3. M. Wu *et al.*, Phylogenomics of the reproductive parasite *Wolbachia* pipientis *w*Mel: A
948 streamlined genome overrun by mobile genetic elements. *PLoS Biol.* **2**, 327-341 (2004).
949 4. J. H. Werren, W. Zhang, L. R. Guo, Evolution and phylogeny of *Wolbachia* - reproductive
950 parasites of arthropods. *Proc. R. Soc. Lond. B* **261**, 55-63 (1995).
951 5. N. Bensaadi-Merchermek, J.-C. Salvado, C. Cagnon, S. Karama, C. Mouchès,
952 Characterization of the unlinked 16S rDNA and 23S-5S rRNA operon of *Wolbachia*
953 *pipientis*, a prokaryotic parasite of insect gonads. *Gene* **165**, 81-86 (1995).
954 6. R. Zug, P. Hammerstein, Still a host of hosts for *Wolbachia*: Analysis of recent data
955 suggests that 40% of terrestrial arthropod species are infected. *PLoS One* **7** (2012).
956 7. K. Hilgenboecker, P. Hammerstein, P. Schlattmann, A. Telschow, J. H. Werren, How many
957 species are infected with *Wolbachia*? - A statistical analysis of current data. *FEMS*
958 *Microbiol. Lett.* **281**, 215-220 (2008).
959 8. F. Rousset, D. Bouchon, B. Pintureau, P. Juchault, M. Solignac, *Wolbachia* endosymbionts
960 responsible for various alterations of sexuality in arthropods. *Proc. R. Soc. Lond. B* **250**,
961 91-98 (1992).
962 9. K. Fenn, M. Blaxter, *Wolbachia* genomes: revealing the biology of parasitism and
963 mutualism. *Trends Parasitol.* **22**, 60-65 (2006).
964 10. R. Stouthamer, J. A. J. Breeuwer, G. D. D. Hurst, *Wolbachia pipientis*: Microbial
965 manipulator of arthropod reproduction. *Annu. Rev. Microbiol.* **53**, 71-102 (1999).
966 11. C. A. Hamm *et al.*, *Wolbachia* do not live by reproductive manipulation alone: infection
967 polymorphism in *Drosophila suzukii* and *D. subpulchrella*. *Mol. Ecol.* **23**, 4871-4885
968 (2014).

969 12. R. Zug, P. Hammerstein, Bad guys turned nice? A critical assessment of *Wolbachia*
970 mutualisms in arthropod hosts. *Biological Reviews* **90**, 89-111 (2015).
971 13. A. R. I. Lindsey, T. Bhattacharya, I. L. G. Newton, R. W. Hardy, Conflict in the intracellular
972 lives of endosymbionts and viruses: A mechanistic look at *Wolbachia*-mediated pathogen-
973 blocking. *Viruses* **10**, 141 (2018).
974 14. E. P. Caragata, H. L. Dutra, P. H. Sucupira, A. G. Ferreira, L. A. Moreira, *Wolbachia* as
975 translational science: controlling mosquito-borne pathogens. *Trends Parasitol.* **37**, 1050-
976 1067 (2021).
977 15. T. Hosokawa, R. Koga, Y. Kikuchi, X. Y. Meng, T. Fukatsu, *Wolbachia* as a bacteriocyte-
978 associated nutritional mutualist. *Proc. Natl. Acad. Sci.* **107**, 769-774 (2010).
979 16. A. C. Gill, A. C. Darby, B. L. Makepeace, Iron necessity: the secret of *Wolbachia*'s
980 success? *PLoS Negl. Trop. Dis.* **8**, e3224 (2014).
981 17. N. Kremer *et al.*, *Wolbachia* interferes with ferritin expression and iron metabolism in
982 insects. *PLoS Path.* **5**, e1000630 (2009).
983 18. V. Geoghegan *et al.*, Perturbed cholesterol and vesicular trafficking associated with
984 dengue blocking in *Wolbachia*-infected *Aedes aegypti* cells. *Nat. Commun.* **8**, 526 (2017).
985 19. J.-F. Ju *et al.*, *Wolbachia* supplement biotin and riboflavin to enhance reproduction in
986 planthoppers. *The ISME journal* **14**, 676-687 (2020).
987 20. A. R. Lindsey, T. Bhattacharya, R. W. Hardy, I. L. Newton, *Wolbachia* and virus alter the
988 host transcriptome at the interface of nucleotide metabolism pathways. *mBio* **12** (2021).
989 21. I. L. Newton, D. W. Rice, The Jekyll and Hyde symbiont: could *Wolbachia* be a nutritional
990 mutualist? *J. Bacteriol.* **202** (2020).
991 22. L. W. Beukeboom, Size matters in insects–an introduction. *Entomol. Exp. Appl.* **166**, 2-3
992 (2018).
993 23. C. Dmitriew, L. Rowe, The effects of larval nutrition on reproductive performance in a food-
994 limited adult environment. *PLoS One* **6**, e17399 (2011).

995 24. B. Taborsky, The influence of juvenile and adult environments on life-history trajectories.
996 *Proc. R. Soc. Lond. B* **273**, 741-750 (2006).
997 25. J. H. Werren, D. M. Windsor, *Wolbachia* infection frequencies in insects: Evidence of a
998 global equilibrium? *Proc. R. Soc. Lond. B* **267**, 1277-1285 (2000).
999 26. W. Huang *et al.*, Natural variation in genome architecture among 205 *Drosophila*
1000 *melanogaster* Genetic Reference Panel lines. *Genome Res.* **24**, 1193-1208 (2014).
1001 27. M. W. Jones, L. C. Fricke, C. J. Thorpe, L. O. V. Esch, A. R. I. Lindsey, Infection dynamics
1002 of cotransmitted reproductive symbionts are mediated by sex, tissue, and development.
1003 *Appl. Environ. Microbiol.* **88**, e00529-00522 (2022).
1004 28. G. dos Santos *et al.*, FlyBase: introduction of the *Drosophila melanogaster* Release 6
1005 reference genome assembly and large-scale migration of genome annotations. *Nucleic*
1006 *Acids Res.* **43**, D690-D697 (2014).
1007 29. B. Li, C. N. Dewey, RSEM: accurate transcript quantification from RNA-Seq data with or
1008 without a reference genome. *BMC Bioinformatics* **12**, 323 (2011).
1009 30. A. Dobin *et al.*, STAR: ultrafast universal RNA-seq aligner. *Bioinformatics* **29**, 15 - 21
1010 (2013).
1011 31. R Core Team (2014) R: A language and environment for statistical computing. (URL
1012 http://www.R-project.org/, R Foundation for Statistical Computing, Vienna, Austria).
1013 32. C. Soneson, M. I. Love, M. D. Robinson, Differential analyses for RNA-seq: transcript-
1014 level estimates improve gene-level inferences. *F1000Research* **4** (2015).
1015 33. M. D. Robinson, D. J. McCarthy, G. K. Smyth, edgeR: a Bioconductor package for
1016 differential expression analysis of digital gene expression data. *Bioinformatics* **26**, 139-
1017 140 (2010).
1018 34. D. J. McCarthy, Y. Chen, G. K. Smyth, Differential expression analysis of multifactor RNA-
1019 Seq experiments with respect to biological variation. *Nucleic Acids Res.* **40**, 4288-4297
1020 (2012).

1021 35. A. Yim *et al.*, mitoXplorer, a visual data mining platform to systematically analyze and
1022 visualize mitochondrial expression dynamics and mutations. *Nucleic Acids Res.* **48**, 605-
1023 632 (2020).
1024 36. F. Marchiano, M. Haering, B. H. Habermann, The mitoXplorer 2.0 update: integrating and
1025 interpreting mitochondrial expression dynamics within a cellular context. *Nucleic Acids*
1026 *Res.* **50**, W490-W499 (2022).
1027 37. Y. Hu *et al.*, PANGEA: a new gene set enrichment tool for *Drosophila* and common
1028 research organisms. *Nucleic Acids Res.* **51**, W419-W426 (2023).
1029 38. N. T. Doncheva, J. H. Morris, J. Gorodkin, L. J. Jensen, Cytoscape stringApp: Network
1030 analysis and visualization of proteomics data. *Journal of Proteome Research* (2018).
1031 39. P. Shannon *et al.*, Cytoscape: a software environment for integrated models of
1032 biomolecular interaction networks. *Genome Res.* **13**, 2498-2504 (2003).
1033 40. F. Gutzwiller *et al.*, Dynamics of *Wolbachia pipientis* gene expression across the
1034 *Drosophila melanogaster* life cycle. *G3: Genes| Genomes| Genetics* **5**, 2843-2856 (2015).
1035 41. B. R. Graveley *et al.*, The developmental transcriptome of *Drosophila melanogaster*.
1036 *Nature* **471**, 473-479 (2011).
1037 42. M. Chung *et al.*, A meta-analysis of *Wolbachia* transcriptomics reveals a stage-specific
1038 *Wolbachia* transcriptional response shared across different hosts. *G3: Genes, Genomes,*
1039 *Genetics* **10**, 3243-3260 (2020).
1040 43. L. C. Fricke, A. R. Lindsey, Identification of parthenogenesis-inducing effector proteins in
1041 *Wolbachia*. *Genome Biol. Evol.*, evae036 (2024).
1042 44. M. Lechner *et al.*, Proteinortho: detection of (co-) orthologs in large-scale analysis. *BMC*
1043 *Bioinformatics* **12**, 1-9 (2011).
1044 45. R. Kolde, M. R. Kolde, Package 'pheatmap'. *R package* **1**, 790 (2015).
1045 46. S. X. Ge, D. Jung, R. Yao, ShinyGO: a graphical gene-set enrichment tool for animals and
1046 plants. *Bioinformatics* **36**, 2628-2629 (2020).

1047 47. S. Bainbridge, M. Bownes, Staging the metamorphosis of *Drosophila melanogaster*.
1048 *Journal of Embryology and Experimental Morphology* **66**, 57-80 (1981).
1049 48. T. Reis, Effects of synthetic diets enriched in specific nutrients on *Drosophila* development,
1050 body fat, and lifespan. *PLoS One* **11**, e0146758 (2016).
1051 49. F. Demontis, N. Perrimon, Integration of Insulin receptor/Foxo signaling and dMyc activity
1052 during muscle growth regulates body size in *Drosophila*. (2009).
1053 50. L. Moss-Taylor, A. Upadhyay, X. Pan, M.-J. Kim, M. B. O'Connor, Body size and tissue-
1054 scaling is regulated by motoneuron-derived activinß in *Drosophila melanogaster*. *Genetics*
1055 **213**, 1447-1464 (2019).
1056 51. S. P. Bainbridge, M. Bownes, Staging the metamorphosis of Drosophila melanogaster.
1057 *Development* **66**, 57-80 (1981).
1058 52. K. J. Livak, T. D. Schmittgen, Analysis of relative gene expression data using real-time
1059 quantitative PCR and the 2− ΔΔCT method. *methods* **25**, 402-408 (2001).
1060 53. J. E. Cox, C. S. Thummel, J. M. Tennessen, Metabolomic studies in *Drosophila*. *Genetics*
1061 **206**, 1169-1185 (2017).
1062 54. H. Li, J. M. Tennessen, Preparation of *Drosophila* larval samples for gas chromatography-
1063 mass spectrometry (GC-MS)-based metabolomics. *JoVE (Journal of Visualized*
1064 *Experiments)*, e57847 (2018).
1065 55. T. Nemkov, J. A. Reisz, S. Gehrke, K. C. Hansen, A. D'Alessandro, High-throughput
1066 metabolomics: isocratic and gradient mass spectrometry-based methods. *High-*
1067 *Throughput Metabolomics: Methods and Protocols*, 13-26 (2019).
1068 56. D. Bates, M. Maechler, B. Bolker, S. Walker, lme4: Linear mixed-effects models using
1069 Eigen and S4. *R package version* **1** (2014).
1070 57. J. Oksanen *et al.*, vegan: Community Ecology Package. R package version 2.0-1.
1071 http://CRAN.R-project.org/package=vegan (2015).

1072 58. J. Xia, N. Psychogios, N. Young, D. S. Wishart, MetaboAnalyst: a web server for
1073 metabolomic data analysis and interpretation. *Nucleic Acids Res.* **37**, W652-W660 (2009).
1074 59. T. Bhattacharya, I. L. G. Newton, R. W. Hardy, Wolbachia elevates host methyltransferase
1075 expression to block an RNA virus early during infection. *PLoS Path.* **13**, e1006427 (2017).
1076 60. A. Sasaki, T. Nishimura, T. Takano, S. Naito, S. K. Yoo, *white* regulates proliferative
1077 homeostasis of intestinal stem cells during ageing in *Drosophila*. *Nature Metabolism* **3**,
1078 546-557 (2021).
1079 61. A. J. Hilliker, B. Duyf, D. Evans, J. P. Phillips, Urate-null rosy mutants of *Drosophila*
1080 *melanogaster* are hypersensitive to oxygen stress. *Proc. Natl. Acad. Sci.* **89**, 4343-4347
1081 (1992).
1082 62. M. Conrad, H. Sato, The oxidative stress-inducible cystine/glutamate antiporter, system
1083 xc−: cystine supplier and beyond. *Amino Acids* **42**, 231-246 (2012).
1084 63. R. Lugo-Huitrón *et al.*, On the antioxidant properties of kynurenic acid: free radical
1085 scavenging activity and inhibition of oxidative stress. *Neurotoxicol. Teratol.* **33**, 538-547
1086 (2011).
1087 64. K. Afshar, P. Gönczy, S. DiNardo, S. A. Wasserman, *fumble* encodes a pantothenate
1088 kinase homolog required for proper mitosis and meiosis in *Drosophila melanogaster*.
1089 *Genetics* **157**, 1267-1276 (2001).
1090 65. M. Gerth, C. Bleidorn, Comparative genomics provides a timeframe for *Wolbachia*
1091 evolution and exposes a recent biotin synthesis operon transfer. *Nat. Micro.* **2**, 16241
1092 (2016).
1093 66. D. Currin-Ross *et al.*, The metabolic response to infection with *Wolbachia* implicates the
1094 insulin/insulin-like-growth factor and hypoxia signaling pathways in *Drosophila*
1095 *melanogaster*. *Frontiers in Ecology and Evolution* **9**, 623561 (2021).

1096 67. J. C. Brownlie *et al.*, Evidence for metabolic provisioning by a common invertebrate
1097 endosymbiont, *Wolbachia pipientis,* during periods of nutritional stress. *PLoS Path.* **5**,
1098 e1000368 (2009).
1099 68. E. Rancès, Y. H. Ye, M. Woolfit, E. A. McGraw, S. L. O'Neill, The relative importance of
1100 innate immune priming in *Wolbachia*-mediated dengue interference. *PLoS Path.* **8**,
1101 e1002548 (2012).
1102 69. N. Camara, C. Whitworth, M. Van Doren, The creation of sexual dimorphism in the
1103 *Drosophila* soma. *Current Topics in Developmental Biology* **83**, 65-107 (2008).
1104 70. N. A. Broderick, B. Lemaitre, Gut-associated microbes of *Drosophila melanogaster*. *Gut*
1105 *Microbes* **3**, 307-321 (2012).
1106 71. D. N. Lesperance, N. A. Broderick, Microbiomes as modulators of *Drosophila*
1107 *melanogaster* homeostasis and disease. *Current Opinion in Insect Science* **39**, 84-90
1108 (2020).
1109 72. D. Falk, R. Bellamy, M. el Kouni, N. F, A genetic and dietary study of the physiology of
1110 pyrimidine synthesis in *Drosophila melanogaster*. *J. Insect Physiol.* **26**, 735-740 (1980).
1111 73. A. Bajgar, T. Dolezal, Extracellular adenosine modulates host-pathogen interactions
1112 through regulation of systemic metabolism during immune response in Drosophila. *PLoS*
1113 *Path.* **14**, e1007022 (2018).
1114 74. M. Fang, Y. Chai, G. Chen, H. Wang, B. Huang, N6-(2-hydroxyethyl)-adenosine exhibits
1115 insecticidal activity against Plutella xylostella via adenosine receptors. *PLoS One* **11**,
1116 e0162859 (2016).
1117 75. J. H. Schroader *et al.*, Disease-associated inosine misincorporation into RNA hinders
1118 translation. *Nucleic Acids Res.* **50**, 9306-9318 (2022).
1119 76. D. R. Evans, H. I. Guy, Mammalian pyrimidine biosynthesis: fresh insights into an ancient
1120 pathway. *J. Biol. Chem.* **279**, 33035-33038 (2004).

1121 77. J.-J. Chen, M. E. Jones, The cellular location of dihydroorotate dehydrogenase: relation
1122 to de novo biosynthesis of pyrimidines. *Archives of Biochemistry and Biophysics* **176**, 82-
1123 90 (1976).
1124 78. J. M. Rawls, Genetic complementation and enzyme correlates at the locus encoding the
1125 last two steps of de novo pyrimidine biosynthesis in *Drosophila melanogaster*. *Molecular*
1126 *and General Genetics MGG* **184**, 174-179 (1981).
1127 79. M. Löffler, E. A. Carrey, W. Knecht, The pathway to pyrimidines: The essential focus on
1128 dihydroorotate dehydrogenase, the mitochondrial enzyme coupled to the respiratory
1129 chain. *Nucleosides Nucleotides Nucl. Acids* **39**, 1281-1305 (2020).
1130 80. L. Brennan, J. Haukedal, J. Earle, B. Keddie, H. Harris, Disruption of redox homeostasis
1131 leads to oxidative DNA damage in spermatocytes of *Wolbachia*-infected *Drosophila*
1132 *simulans*. *Insect Mol. Biol.* **21**, 510-520 (2012).
1133 81. R. Zug, P. Hammerstein, *Wolbachia* and the insect immune system: what reactive oxygen
1134 species can tell us about the mechanisms of *Wolbachia*–host interactions. *Frontiers in*
1135 *Microbiology* **6**, 1201 (2015).
1136 82. X. Pan *et al.*, *Wolbachia* induces reactive oxygen species (ROS)-dependent activation of
1137 the Toll pathway to control dengue virus in the mosquito *Aedes aegypti*. *Proc. Natl. Acad.*
1138 *Sci.* **109**, E23-E31 (2012).
1139 83. D. Monnin *et al.*, Influence of oxidative homeostasis on bacterial density and cost of
1140 infection in *Drosophila*–*Wolbachia* symbioses. *J. Evol. Biol.* **29**, 1211-1222 (2016).
1141 84. Z. S. Wong, J. C. Brownlie, K. N. Johnson, Oxidative stress correlates with *Wolbachia*-
1142 mediated antiviral protection in *Wolbachia-Drosophila* associations. *Appl. Environ.*
1143 *Microbiol.* **81**, 3001-3005 (2015).
1144 85. L. J. Brennan, B. A. Keddie, H. R. Braig, H. L. Harris, The endosymbiont *Wolbachia*
1145 *pipientis* induces the expression of host antioxidant proteins in an *Aedes albopictus* cell
1146 line. *PLoS One* **3** (2008).

1147 86. A. C. Darby *et al.*, Analysis of gene expression from the *Wolbachia* genome of a filarial
1148 nematode supports both metabolic and defensive roles within the symbiosis. *Genome*
1149 *Res.* **22**, 2467-2477 (2012).
1150 87. R. Kumar, R. Srivastava, R. K. Singh, A. Surolia, D. N. Rao, Activation and inhibition of
1151 DNA methyltransferases by S-adenosyl-L-homocysteine analogues. *Bioorganic &*
1152 *Medicinal Chemistry* **16**, 2276-2285 (2008).
1153 88. T. Bhattacharya *et al.*, Differential viral RNA methylation contributes to pathogen blocking
1154 in *Wolbachia*-colonized arthropods. *PLoS Path.* **18**, e1010393 (2022).
1155 89. S. Layalle, N. Arquier, P. Léopold, The TOR pathway couples nutrition and developmental
1156 timing in *Drosophila*. *Dev. Cell* **15**, 568-577 (2008).
1157 90. C. Géminard, E. J. Rulifson, P. Léopold, Remote control of insulin secretion by fat cells in
1158 Drosophila. *Cell Metabolism* **10**, 199-207 (2009).
1159 91. J. Colombani *et al.*, A nutrient sensor mechanism controls *Drosophila* growth. *Cell* **114**,
1160 739-749 (2003).
1161 92. M. J. Texada, T. Koyama, K. Rewitz, Regulation of body size and growth control. *Genetics*
1162 **216**, 269-313 (2020).
1163 93. A. R. I. Lindsey, Sensing, Signaling, and Secretion: A review and analysis of systems for
1164 regulating host interaction in *Wolbachia*. *Genes* **11**, 813 (2020).
1165 94. K.-O. Cho, G.-W. Kim, O.-K. Lee, *Wolbachia* bacteria reside in host Golgi-related vesicles
1166 whose position is regulated by polarity proteins. *PLoS One* **6**, e22703 (2011).
1167 95. P. M. White *et al.*, Reliance of *Wolbachia* on high rates of host proteolysis revealed by a
1168 genome-wide RNAi screen of *Drosophila* cells. *Genetics* **205**, 1473-1488 (2017).
1169 96. L. R. Serbus *et al.*, The impact of host diet on *Wolbachia* titer in *Drosophila*. *PLoS Path.*
1170 **11**, e1004777 (2015).

1171 97. N. A. Moran, G. R. Plague, J. P. Sandström, J. L. Wilcox, A genomic perspective on nutrient
1172 provisioning by bacterial symbionts of insects. *Proc. Natl. Acad. Sci.* **100**, 14543-14548
1173 (2003).
1174 98. N. A. Moran, Symbiosis. *Curr. Biol.* **16**, R866-871 (2006).
1175